



Integration of assessment-methods for wave renewable energy: Resource and installation feasibility

Ophelie Choupin ^a, B. Del Río-Gamero ^{b,*}, Julieta Schallenberg-Rodríguez ^b, Pablo Yáñez-Rosales ^b

^a Institute of Oceanography of the University of São Paulo, São Paulo, Brazil

^b Industrial and Civil Engineering School. Universidad de Las Palmas de Gran Canaria, Las Palmas de Gran Canaria, Spain

ARTICLE INFO

Article history:

Received 9 July 2021

Received in revised form

14 October 2021

Accepted 9 December 2021

Available online 16 December 2021

Keywords:

Wave energy

Canary islands

Wave metrics and indices

Wave resource

Operation & maintenance

Geographical information system (GIS)

ABSTRACT

As wave renewables can be a cornerstone in the energy mix framework necessary for a green energy transition, a new integrated model is introduced to assess coastal locations and wave resource potential for renewable installations based on: (A) wave resource metrics and indices, and (B) geographical analyses. The Canary archipelago (Spain) is a relevant case study due to its different islands' interactions and its human-related/environmental (including fauna/flora) restrictions. With respect to (A), 63 approaches (for 40 parameters) were investigated regarding their relevancy, complementarity and representativeness, to reduce them to a critical 9 final key performance indicators for the wave resource (power, direction, harshness and availability, amongst others). These were then strategically integrated to conduct the actual wave resource analysis. The restrictions assessed in (B) resulted in the distinction of most and least restrictive scenarios. The areas available for renewable installation according to (B) were then merged with the resource assessment performed in (A). Results highlight the archipelago's appeal for renewable installation, with the islands displaying a complex high-potential coverage partially located in the most restrictive scenario.

© 2021 The Authors. Published by Elsevier Ltd. This is an open access article under the CC BY-NC-ND license (<http://creativecommons.org/licenses/by-nc-nd/4.0/>).

1. Introduction

In the need to transit to a more mixed renewable energy framework [1–3], marine renewables (e.g. wind, wave, and tidal) have been shown to compensate one another in terms of flexibility and variability [4,5] ensuring less disruptive transmissions. The global wave energy resource is about 3 TW [6]. Additionally, wave energy converters (WECs) installed in combination with other marine renewables have the potential to increase structural stability and lower installation and operating and maintenance (O&M) costs [7,8]. The mix of marine renewables could solve the lack of energy access of coastal regions with limited land space [9]. Where present offshore wind is less costly, factors such as (a) low visual impact compared to other renewable technologies, (b) high predictability, density, and stability motivate the wave resource exploitation [10].

Essentially, wave assessment consists of determining the significant wave height, peak/energy wave period and wave energy potential per unit crest length [11]. Yet, the wave direction influences wave energy harvesting, so statistical models for the joint distribution of these four parameters are needed to fully characterise the wave climate [12], particularly for the wide range of wave direction-dependent WECs [13]. Furthermore, location assessment works tend only to investigate the wave resource energy potential and inter- and intra-annual variability, and a broad range of indices and metrics (including wave resource harshness, O&M, and availability assessment) [14–16] is in constant development, which increases the complexity of wave resource assessment. Therefore, an analysis of these Wave-Resource Key Performance Indicators (WR-KPIs) is necessary to understand their relevancy, complementarity, and representativeness to thereby reduce the time-consuming analysis.

The wave resource availability may support energy production of islands [17], including the Canary Islands (Spain, Fig. 1). While this region is generally characterised by swell and minimum extreme wave conditions that favour WEC installations [14,18,19], an evaluation of the entire coast is required to pinpoint ideal

* Corresponding author.

E-mail address: beatriz.delrio@ulpgc.es (B. Del Río-Gamero).

locations. Several studies have been conducted to evaluate the seven islands wave resource independently. The majority used WAM, a broadly validated third-generation spectral numerical model. However, studies often use different forcing-databases (HYPOCAS, WANA, NECP, NCAR) [20–23], many are not within the recommended minimum 10-year period by the International Electrotechnical Commission [24], the spacing resolution often differs, and area restrictions are not taken into account. Veigas et al. [25] also identified it as a requirement. These gaps in addition to the lack of inclusive WR-KPIs assessment are visible in the literature provided in Fig. 1 that summarizes the related research that has been conducted for different Canary islands. No study assess the archipelago wave resource as a whole.

This work uses a 27-year consistent gridded model over the Canary archipelago and aims to develop two methods for (A) wave resource analysis and (B) marine area installation selection. To conduct (A), WR-KPIs are surveyed and completed to reduce their number, and a method is developed to integrate the remaining ones. In (B), a geographical feasibility study of the coasts and their particular features is carried out by expanding the methodology of Bertram et al. [26], including geographical dataset restrictions for marine renewable installations, which are compiled in different

Geographic Information System (GIS) layers and two restrictive scenarios are distinguished and discussed. Finally, the mapping of (A) and (B) are combined to draw the final conclusions on potential areas (i.e. sweetspots) for installing marine renewable facilities, highlighting areas of particular interest for WECS.

2. Framework of the method

Fig. 2 displays the framework on which (A) and (B) are based to obtain the final “wave resource and installation potential”. Firstly (Fig. 2A), wave data are acquired, validated and processed. The wave data are obtained from historical hindcast databases, among other sources. The analysis of these parameters is followed by their use in the evaluation of the WR-KPIs to assess their level of importance and representation of the whole, for the holistic understanding of the wave climate. The objective is to decrease the level of bias and uncertainty in the analysis to obtain the final WR-KPIs selection and elaborate a method for their integration in the next section. In parallel, a critical analysis of geographical areas restrictions must be undertaken when identifying suitable regions for wave energy harvesting (Fig. 2B).



Fig. 1. Summary of the analysis of the wave resource in the Canary archipelago researches.

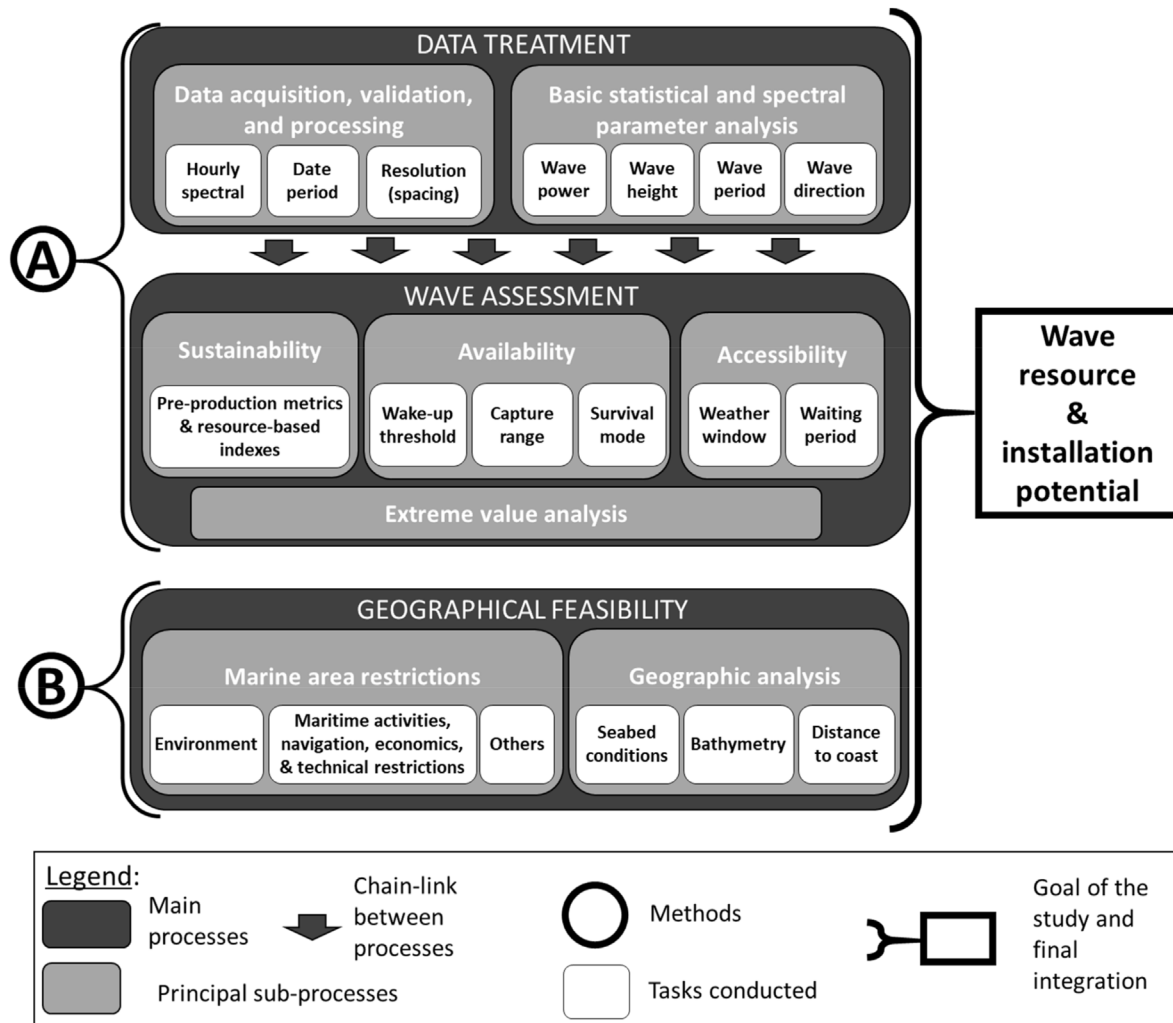


Fig. 2. Framework flow chart for assessing wave resource and installation potential.

2.1. Data treatment

2.1.1. Data acquisition and processing

A multi-year high-resolution wave reanalysis product for the Iberian Biscay Ireland [27] from the Copernicus Marine Environment Monitoring Service (CMEMS) [28] is used. The dataset covers 1993–2019 (1 h temporal and ~5 km spatial resolutions) of wave data [29]. It has been validated including for the Canary archipelago [30]. Fig. 3 shows the mesh covering the Canary Islands and the water depth obtained from the ETOPO bathymetry dataset [31].

2.1.2. Wave data: basic statistical and spectral parameters analysis

First, the significant wave heights (statistical H_s , mean wave height of the largest third of the wave heights in the sea state [32], and spectral $Hm_0 = 4(m_0^{1/2})$, with m_0 the first moment of the wave spectrum) are assumed to be the same, following IEC technical specifications [33,34]. Secondly, the peak period (T_p) is associated with the peak of the wave energy spectrum, with the energy period (T_e) being the period of a sinusoidal wave that would carry the same energy as the sea state [35]. Thirdly, as a crucial parameter for wave farms and direction-dependent WECs [36,37], the peak direction (θ_p) associated with the wave peak period has also been downloaded from the CMEMS. This has been done for simplicity as most wave direction-dependent WECs are currently expressed by

means of θ_p [36,37]. Hence, although this study originally considered the mean wave direction, it is not shown. Finally, the wave power flux J (kW/m) is determined using Eq. (1) [38,39], with g the gravitational acceleration (9.81 m/s^2), ρ the seawater density ($\sim 1.027 \text{ kg/m}^3$), and c the wave celerity (m/s). Following the cases of deep, intermediary, and shallow water, c and thereby Eq. (1) have been simplified as per Table 1 (following [40,41]), with L (m) the wavelength, h (m) the water depth, and the wavenumber, k (–) obtained from Eq. (3) [40]. L is calculated using Eq. (2) [42] solved following [43].

$$J = \frac{\rho g H_s^2 c}{16} \left(1 + \frac{2kh}{\sinh(2kh)} \right)$$

$$L = \frac{g T_e^2}{2\pi} \tanh\left(\frac{2\pi h}{L}\right)$$

$$k = \frac{2\pi}{L}$$

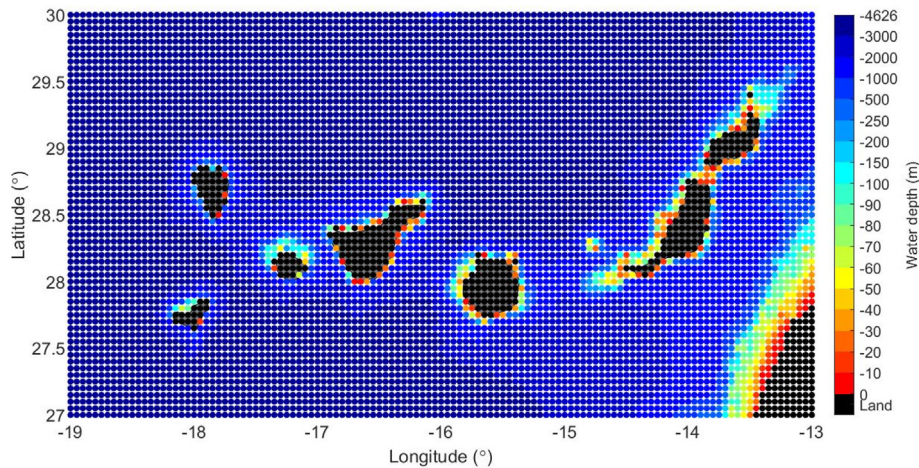


Fig. 3. Mesh resolution and bathymetry. Black circles are land cells.

Table 1

Wave celerity and wave power flux equations in function of the water depth ranges based on [40].

Water depth [reference]	Water depth ranges	Wave celerity (m/s)	Full wave power flux equation (kW/m)
Deep [44,45]	$\frac{h}{L} > \frac{1}{2}$	$c = \frac{gT_e}{2\pi}$	$J = \frac{\rho g^2}{64\pi} H_s^2 T_e$
Intermediary [43,46]	$\frac{1}{2} > \frac{h}{L} > \frac{1}{20}$	$c = \frac{gT_e}{2\pi} \tanh(kh)$	$J = \frac{\rho g^2}{64\pi} H_s^2 T_e \tanh(kh) \left(1 + \frac{2kh}{\sinh(2kh)}\right)$
Shallow [40]	$\frac{h}{L} < \frac{1}{20}$	$c = \sqrt{gh}$	$J = \frac{\rho g}{32\pi} H_s^2 \sqrt{gh} \left(1 + \frac{2kh}{\sinh(2kh)}\right)$

2.2. Wave assessment

2.2.1. Sustainability metrics and indices for wave resource assessment

Multiple works have developed WR-KPIs to help understand marine resources [14,16,47–50]. Recently Guillou et al. [16] reviewed and classified WR-KPIs. As this work focuses on wave resource analysis, only pre-production metrics and resource-based indices are considered. Aside from the mean and aggregated mean wave power, other basic statistics (median, standard deviations, kurtosis, skewness, and percentiles, to cite a few) [11,51] were considered to assess the results but are not presented as out of this study's scope focused on elaborated WR-KPIs. The new Wave Period Exploitation Development Index (WaPEDI) is developed based on [49,50] to complete wave period analyses. Additionally, lacking wave direction analyses are compensated using the mean wave peak direction and its validation range obtained using the CircStat package [52], closely following the method from [53] originally applied to wind renewables. Table 2 describes the most important WR-KPIs (for more detailed information, please refer to Appendix A).

2.2.2. Extreme value analysis

Extreme value analyses (EVAs) estimate the return wave height that helps to understand the wave conditions harshness and thereby the maximum constraints that the WEC will need to support. The wave height distribution is reduced to the maximum values using the peak-over-threshold (POT) method, and ensuring the average 3-days between the data following the identically independent distribution (i.i.d.) [61,62]. Following the method of [63], from the obtained discontinuous distribution, its most appropriate fitting-curve, i.e. Weibull [64] amongst others [65,66],

is utilised to estimate the return wave height for a given return period. Despite the consideration of other EVA parameters (see Appendix A), this study focuses on the return wave height for its direct inclusion in recent most developed WEC-location pairing cost-independent indexes using return periods of 30 [48] and 100 years [67]. This mathematical method could similarly apply to the wave period, but parameters such as the design wave period are often calculated in function of EVA's wave height [68]. Extreme wave periods are widely omitted because they mainly affect the amount of available energy without representing much direct threat to the structure [69]. Generally speaking, long waves with high wave heights rarely happen in high energetic wave climates [70]. All together, these lead back to the extreme wave height analysis [69] relating structure-loads and extra costs.

2.2.3. Availability and accessibility

Guanche et al. [15] provided conservative ranges to quantify availability regarding WEC wake-up thresholds (Table 3). Since the availability is typically defined as the percentage of time that the device can operate, if the resource is sufficient and that cases of low wave energy are generally not counted against its availability, these 0.5–4 m thresholds have been retained.

Accessibility, the percentage of time which a device can be accessed for O&M ($H_s < 1.5$ m), is the basis for weather window analyses related to O&M feasibility [15,67]. The minimum weather window time of 6–12 h up to 24 and 48 h was assessed, as in other studies [15,71]. To ensure that O&M is possible during daylight hours, the window analysis is not performed on an hourly basis but rather over a 1–7 day range (5–7-day enabling long-period activities including overhaul/mid-life refit). Consequently, the periods of inaccessibility between the weather windows, known as waiting periods, are also analysed.

Table 2
Equations of the sustainability metrics and indices for wave resource assessment.

Parameters and reference	Formula	Definition	Expected range of values and objective value
Pre-production metrics			
Coefficient of variation [CoV, non-dimensional] [48,54]	$CoV = \frac{\sigma_P}{P_{mean}}$	(4) Amount of variability with respect to the mean value obtained by dividing the standard deviation of P (σ_P) by the mean available wave power (P_{mean}) over the period considered (normally several decades). It is worth noting that CoV has also been applied to other variables that include the significant wave height (CoV_{Hm0}) [48] and the wave peak period (CoV_{Tp}) [55].	$CoV \geq 0$ Low (for low variability)
Inverse of coefficient of variation [CoV^{-1} , non-dimensional] [51]	$CoV^{-1} = \frac{P_{mean}}{\sigma_P} = \frac{1}{CoV}$	(5) Inverses CoV to obtain a metric that is positively proportional to the level of the power and inversely proportional to its variability. Originally applied to the wave power, this study also extends its application to the significant wave height (CoV^{-1}_{Hm0}) and peak period (CoV^{-1}_{Tp}).	$CoV^{-1} \geq 0$ High (for low variability)
Annual variability index [AVI, non-dimensional] [56]	$AVI = \frac{P_{A1} - P_{A2}}{P_{year}}$	(6) Intra-annual differentiations of the resource. P_{year} is the annual mean wave power, and PA1 and PA2 the mean available wave powers for the most and the least energetic years, respectively.	$AVI \geq 0$ Low (for low annual variability)
Seasonal variability index [SVI, non-dimensional] [56]	$SVI = \frac{P_{S1} - P_{S2}}{P_{year}}$	(7) Intra-seasonal differentiations of the resource. P_{year} is the annual mean wave power, and P_{S1} and P_{S2} the mean available wave powers for the most and least energetic seasons, respectively.	$SVI \geq 0$ Low (for low seasonal variability)
Monthly variability index [MVI, non-dimensional] [56]	$MVI = \frac{P_{M1} - P_{M2}}{P_{year}}$	(8) Intra-monthly differentiations of the resource. P_{year} is the annual mean wave power, and P_{M1} and P_{M2} the mean available wave powers for the most and least energetic months, respectively.	$MVI \geq 0$ Low (for low monthly variability)
Rate of change [RC, kW/m/s] [49]	$RC = \frac{\Delta P}{\Delta T}$	(9) Estimates the persistence of statistical parameters of wave energy (in the case, wave power ΔP) over their time difference (ΔT). In general, RC is obtained over aggregated values, for instance the annual mean of the wave power flux, and in such cases ΔT is the number of considered years.	$RC \in \mathbb{R}$ N/A (if RC is positive, the wave power flux seems to increase over the considered duration and vice versa)
Annual-mean rate of change [ROC, kW/m/year] [57]	$P_{linear}(Y) = ROC \cdot Y + S2_{year}$	(10) The linear regression slope coefficient of the curve consisting of the annual mean wave power flux (P_{linear}), with Y the year, S2 the offset coefficient of the affine function ($ROC \cdot Y + S2_{year}$). ROC provides the increasing or decreasing wave power trend inter-annually.	$ROC \in \mathbb{R}$ N/A (if ROC is positive, the annual mean wave power flux seems to increase and vice versa)
Resource-based indices			
Optimum Hotspot Identifier [OHI, kW/m] [58]	$OHI = \frac{P_{year} \cdot F(P > 2kWm^{-1})}{MVI}$	(11) Shows the most suitable location prescribed by the annual mean wave power (P_{year}) and its frequency of waves greater than 2 kW/m as suitable for wave energy harvesting, versus monthly variability (MVI).	$OHI \geq 0$ High (for a powerful resource with low monthly variations)
Inter-annual variability [t_i , %] [59]	$t_i = \frac{\sigma[E(Y) - (S_1 Y + S_2)]}{AAE_{total}} \cdot 100\%$	(12) Examines inter-annual variation driven by effects of global oscillations (e.g., El Niño), using a standard deviation of a linear regression where S_1 is a slope coefficient, S_2 the offset coefficient of the affine function ($S_1 Y + S_2$), Y the year and AAE_{total} the total theoretical available wave energy in the years considered.	$t_i \geq 0$ Low (for low annual variability)
Seasonal variability [t_s , non-dimensional] [59]	$P_m(M) = J_m(M) \cdot \frac{T_{30years}}{T_{month}}$ $t_s = \frac{[P_m]_{max} - [P_m]_{min}}{J_m}$	(13) Indicates the maximum range of $J_m(M)$, the vector of monthly mean wave power flux, relative to the monthly mean annual wave power P_{year} that is referred to with the J_m factor.	$t_s \geq 0$ Low (for low monthly variability throughout the year)
Sustainability Index for wave power [Slp, non-dimensional] [57]	$P_{annual\ norm} = \frac{P_{year}}{\max(P_{year\ domain})}$ $ROC_{norm} = \frac{Rate\ of\ change}{\max(Rate\ of\ change\ domain)}$ $Slp = \frac{P_{annual\ norm} \cdot \cos(ROC_{norm})}{MVI}$	(14) Includes wave power potential (P_{year}) and long-term inter-annual changes (ROC) to define wave climate sustainability and wave energy by using the normalisation of the variables over the entire considered domain and monthly variations (MVI).	$Slp \geq 0$ High (for highest potential with low variability)
Wave energy development index [WEDI, non-dimensional] [49]	$WEDI = \frac{P_{year}}{J_p}$	(15) Expresses the ratio of annual mean wave power (P_{year}) and the maximum storm wave power (J_p) that every offshore device or structure will have to absorb.	$WEDI \geq 0$ High (for energetic areas with low harsh events)
Wave exploitation index [WEI, non-dimensional] [50]	$WEI = \frac{\overline{H_{rms}}}{\overline{H_{max}}}$	(16) Compares mean and extreme wave heights through a simple ratio using $\overline{H_{rms}}$ as the mean value of the root-mean-square wave height (assuming a Rayleigh	$WEI \geq 0$ High (for great resource exploitation potential)

(continued on next page)

Table 2 (continued)

Parameters and reference	Formula	Definition	Expected range of values and objective value
Pre-production metrics			
Wave Period Exploitation Development Index [WaPEDI, non-dimensional]	$WaPEDI = \frac{\bar{T}_p}{T_{pmax}}$	(17) Similar to WEDI and WEI with application over the wave peak period (T_p), WaPEDI is the mean (\bar{T}_p) over the maximum (T_{pmax}), both obtained over the entire duration.	WaPEDI ≥ 0 High (for more stability of the resource)
Suitability index of the wave resource [SI _{waveR} , %] [14]	$SI_{waveR} = \frac{\left(\left(\frac{t_{Ef}}{\bar{t}} \cdot 2\right) + \frac{t_{Hs}}{\bar{t}} + \frac{t_{Tp}}{\bar{t}}\right)}{4}$	(18) Analyses the percentage of time during which favourable production conditions existed, including safety measures for generic wave devices. For this, the available energy flux (E_f), T_p , and H_s are considered by integrating the time percentages for each element using the weighted mean t_{Ef} , t_{Hs} and t_{Tp} (in hours in this case), that the E_f , H_s and T_p remained above or between certain thresholds in the whole time series.	SI _{waveR} ≥ 0 High (for maximum suitability)
Mean wave peak direction [θ_{p_m} , °] [53]	$\theta_{p_m} = \frac{180}{\pi} \arctan\left(\frac{\sum_{i=1}^n \cos\left(\theta_p \frac{\pi}{180}\right)}{\sum_{i=1}^n \sin\left(\theta_p \frac{\pi}{180}\right)}\right)$	(19) The mean wave direction equation applied to the wave peak direction (θ_p) transferred into the radians using the factor $\frac{\pi}{180}$ provides the mean wave peak direction in grandiant by transferring the arctan output using $\frac{180}{\pi}$. Especially, n is the number of sea states considered during the considered duration. It is worth noting that the median [52] was also considered here, but the mean direction was preferred due to its strong and unique relationship with the mean wave direction validity factor (r_p) further explained below.	$\theta_{p_m} \geq 0$ N/A
Mean wave peak direction validity range (r_p , non-dimensional) [60]	$r_p = \frac{1}{n} \sqrt{\left(\sum_{i=1}^n \cos\left(\theta_p \frac{\pi}{180}\right)\right)^2 + \left(\sum_{i=1}^n \sin\left(\theta_p \frac{\pi}{180}\right)\right)^2}$	(20) r_p is more precisely and technically called the resultant vector length as it represents with its length the representativeness of the mean (peak, in this case) direction. It is worth noting that additional parameters of circular statistics were considered including the standard deviation as in [53] and the variance [52]. Yet, r_p has been selected instead as the most direct representation of the validity range of θ_{p_m} within understandle and comparable between each cell in relation to its easy-to-interpret ranges (see right-hand cell).	$r_p \in [0-1]$ High (for high representation of the mean wave peak direction and thereby low direction varitions of the wave climate)

Table 3
Stipulated values for the analysis of availability and accessibility parameters based on [15,67,71].

	Cut-in threshold (Wake-up threshold)	Operation and maintenance range	WEC operational range	Cut-off threshold (Survival mode)
Hs [m]	0.5<	0–3	0–8	>4

2.3. Geographical feasibility

GIS analyses were conducted using QGIS software [72]. Several protocols for spatial data analysis and project management were used to incorporate government regulations and technical conditions [73]. Additionally, marine area restrictions obtained from the literature were considered and classified according to their objectives (Fig. 2).

2.3.1. Marine area restrictions

2.3.1.1. Environmental restrictions. The Canary Islands involve numerous protected areas, including some important coastal zones restrictions [74]. Table 4 summarizes the regulations and the environmental restrictions that are in force.

Navigation channels for the regular maritime transport of people and goods and other marine activities (e.g. aquaculture, ports, and meteorological instrumentation) comprise additional area restrictions [75]. Maritime transports taking place in international waters are not considered. However, traffic density in port exits and

entrances are analysed following instructions on the MarineTraffic website [76].

2.3.1.2. Other restrictions. Military, airport, telecommunication (e.g. internet and telephony), and electricity facilities can also involve restrictions [75]. Aeronautical easements tend to come from radio signal and operational requirements [77]. It should also be noted that the number of electrical submarine cables along coasts is expected to increase in the coming years [78].

Buffer zones (also to be excluded) may surround restricted areas. Their purpose is to safeguard restricted areas against possible accidents [79]. This is still commonly forgotten in protected area analyses for wave energy applications [80–82]. However, some studies have characterised in detail island coastlines for the implantation of offshore wind turbines [83]. Table 5 identifies the buffer zones considered in the present work. Offshore wind distances have been adjusted forwave renewables. Buffer zones are not applicable to protected environmental areas or aeronautical restrictions.

Table 4
Classification of environmental restrictions. Each Regulation has three restriction domains.

Regulation	Restriction	Definition
Protected Natural Areas (National – Spain)	Marine reserves	Specific measure that contributes to achieving a sustained exploitation of resources of fishing interest, establishing specific protection measures in delimited areas of traditional fishing grounds.
	Important marine bird areas	Areas where a significant part of the population of one or more bird species considered a priority by BirdLife is regularly present.
	Special natural reserve	Areas whose purpose is the preservation of unique habitats, specific species, geological formations or natural ecological processes of special interest and in which human occupation other than scientific, educational and, exceptionally, recreational, or traditional purposes is not compatible.
Natura 2000 Network (European)	Areas of special protection for birds	Its purpose is to ensure the long-term survival of species and habitat types in Europe, helping to halt the loss of biodiversity.
	Important community places in terms of habitats	Places that, in the biogeographic region(s) to which it belongs, contribute significantly to maintaining or re-establishing a type of natural habitat or a species in a favourable conservation status and/or contributing significantly to the maintenance of biological diversity and wealth.
	Special protection areas	Important Community places designated by the Member States by means of a regulatory, administrative and/or contractual act, in which the necessary conservation measures are applied for the maintenance or restoration, in a favourable state of conservation, of natural habitats and/or populations of the species for which the site has been designated.

Maritime activities, navigation, economic, & technical restrictions.

Table 5
Buffer zones in different types of restricted areas.

Restricted areas	Buffer zone [m]
Environmental restrictions	N/A
Main maritime routes	100
Aquaculture concessions	100
Ports	100
Instrumental buoys	100
Military areas	100
Submarine cables	200
Aeronautical	N/A

2.3.2. Geographic analysis

Bathymetry, seabed conditions, and distance from the shoreline are important factors for WEC installation [37]. The shelves around the Canary Islands are steep, which can significantly affect the wave resource [84] and WEC selection (including mooring/anchoring) [37,85,86]. Based on WEC installation depth classifications [87], three bathymetric intervals were considered: 20–50, 50–100 and 100–200 m. Regarding the seabed’s nature, the PLASMAR + project was used to evaluate the different substrates in the archipelago [88]. Finally, WECs should be installed within the country’s territorial waters where the state exercises full sovereignty (jurisdictional waters) [89].

3. Investigation and achievement of the integrated model

This section’s objective is to demonstrate the path to develop the methods for (A) wave resource assessment and (B) location availability for renewable installations. Firstly, aspects related to “Data treatment” and “Wave assessment” (Fig. 2A) are considered to evaluate and reduce the number of WR-KPIs in order to develop an integrated method for wave resource analysis. This is followed by the discussion of “Geographical feasibility” (Fig. 2B) to identify available areas.

3.1. Part (A): Data treatment and wave assessment

Often intra-variations within a year are supposed to be repeated over the years with little change. Therefore, an analysis of WR-KPIs must start with inter-annual variation analyses before intra-annual variations, to understand the level of such an assumption. The other wave assessment aspects follow before a final integration of the WR-KPIs in section 3.1.7.

3.1.1. Annual mean wave power, metrics, and indices

Fig. 4 shows the annual mean wave power (P_{year}) alongside other WR-KPIs related to inter-annual variations. The Canary Islands have an average wave power of 20 kW/m with lower values on the islands extreme southern coast (10 kW/m) [90].

ROC splits the area longitudinally: ROC is high on the left and low on the right with steep increase in the resource between years offshore, and lower increase in the shallow area. Conversely, RC (similarly to P_{year}) cuts the figure latitudinally into an upper part with high positive inter-annual variations. Finally, Slp divides the figure longitudinally, but the low-value section is on the right-hand side due to the ROC’s normalisation and the cosine. Where ROC values are in light blue, the cosine is at its maximum value. Such analyses are important to avoid the possibility of undersizing the renewable farm as the result of increasing annual trends. Generally RC, as well as ROC and P_{year} , and therefore Slp have an opposite offshore-to-nearshore behaviour to AVI and ti . These variations, associated with large and various island shadows, are probably due to mixed phenomena, including north-north-eastern wind fronts and swell as well as the predominant trade winds [91].

Overall, RC_{year} and ROC show whether the wave energy-potential of a location is increasing or decreasing (Table 2) but do not provide information about the island actual resource potential. While P_{year} needs to be high, an excessive value would be beyond the WEC capacity, making it a low boundary metric for location selection. Hence, only AVI, ti , and Slp can be used to assess the inter-annual location potential. There is reasonable agreement between AVI and ti (that need to be low), and the Slp (that needs to be high), especially nearshore where renewables are more likely to be installed. By highlighting high wave power locations with fewer fluctuations, Slp gives more information simultaneously and is, therefore, a good alternative to AVI and ti .

3.1.2. Seasonal and monthly metrics and indices

The islands’ wave resource distribution varies widely seasonally. During winter (December, January, and February), wave potential reaches values above 30 kW/m in the northern regions of most of the islands. In summer (June, July and August), values drop to 9 kW/m on average [90]. Fig. 5 shows the monthly and seasonal WR-KPIs. The worldwide maximum MVI and SVI values approximate 3.6 and 3, respectively [92]. Compared with precise locations, in the eastern Australian shelves, low MVI values (~0.72) are obtained [37], while the Canary Islands are slightly below the 1.75 value of western France [56]. Therefore, there is a non-negligible intra-annual variation especially nearshore, similarly to France.

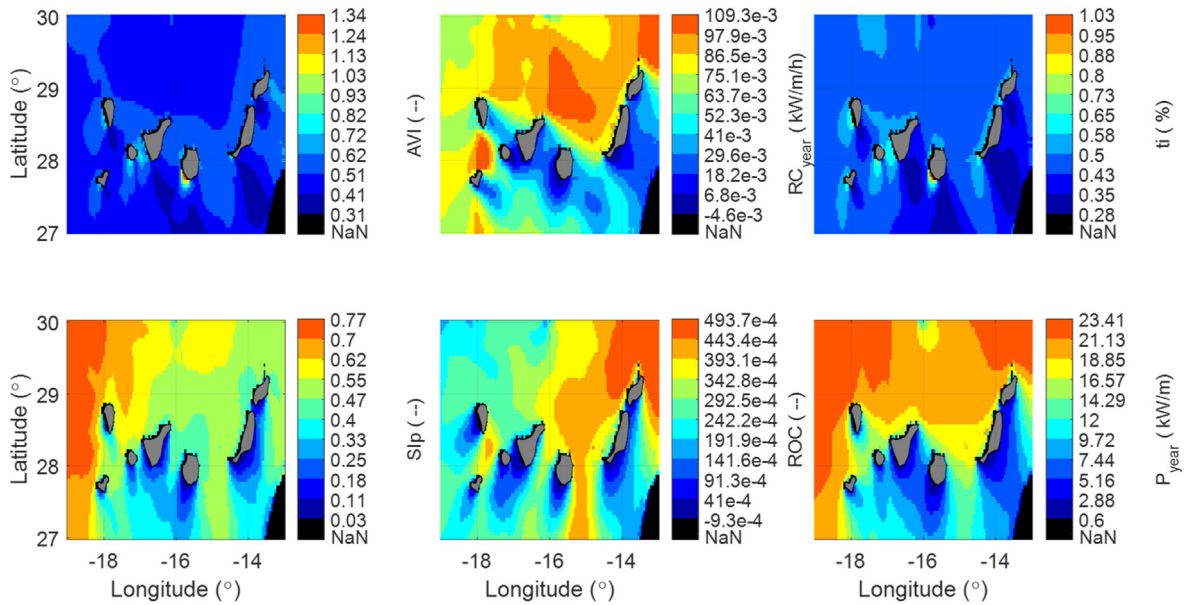


Fig. 4. From left to right and top to bottom: Annual Variation Index (AVI, –), annual mean Rate of Change (RC_{year} , kW/m/h), Inter-annual variability (t_i , %), Sustainability index for the wave power (Slp, –), long-term inter-annual Rate Of Change (ROC, –), and annual mean wave power (P_{year} , kW/m). NaN stands for Not-a-Number (from the Copernicus data), and islands are in grey.

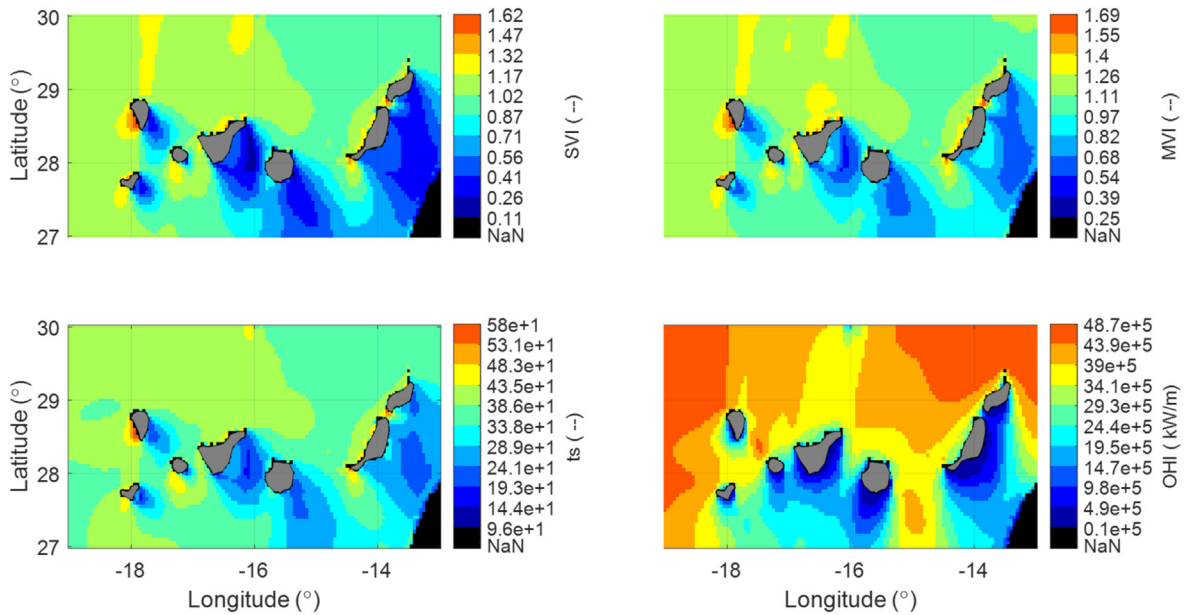


Fig. 5. From left to right and top to bottom: Seasonal Variation Index (SVI, –), Monthly Variation Index (MVI, –), Seasonal Variability (t_s , –), and Optimum Hotspot Identifier (kW/m). NaN stands for Not-a-Number (from the Copernicus data), and islands are in grey.

SVI, MVI, and t_s give similar results. Despite being a function of MVI, Eq. (9), P_{year} (Fig. 4) affects OHI more, except for a couple of locations on the islands’ north where OHI agrees with MVI. Generally, the intra-annual variations longitudinally split the area (similarly to ROC and Slp). ROC seems to have a stronger influence on Slp than the wave power above 2 kW/m on OHI. The impact of MVI is higher for lower P_{year} . Although OHI follows MVI slightly more than Slp, this only slightly affects the results and, as Slp provides more information on the location potential for renewable installation, the use of Slp alone would be sufficient.

3.1.3. Additional wave resource key performance indicators based on the root of the wave parameters

This section focuses on parameters that directly use the hourly time-series as opposed to the above sections based on aggregated data. The left-hand column of Fig. 6 shows the WR-KPIs for wave power flux, the middle column significant wave height, and the right-hand column wave peak period.

CoV of wave power flux is higher than that of the other two (see colour bar scale). Regardless of the strict values and focusing on the colour-spread, CoV_{Hm0} variations’ coverage is larger than those of CoV. Thus, CoV_{Tp} (more uniform than CoV_{Hm0}) stabilises CoV_{Hm0} .

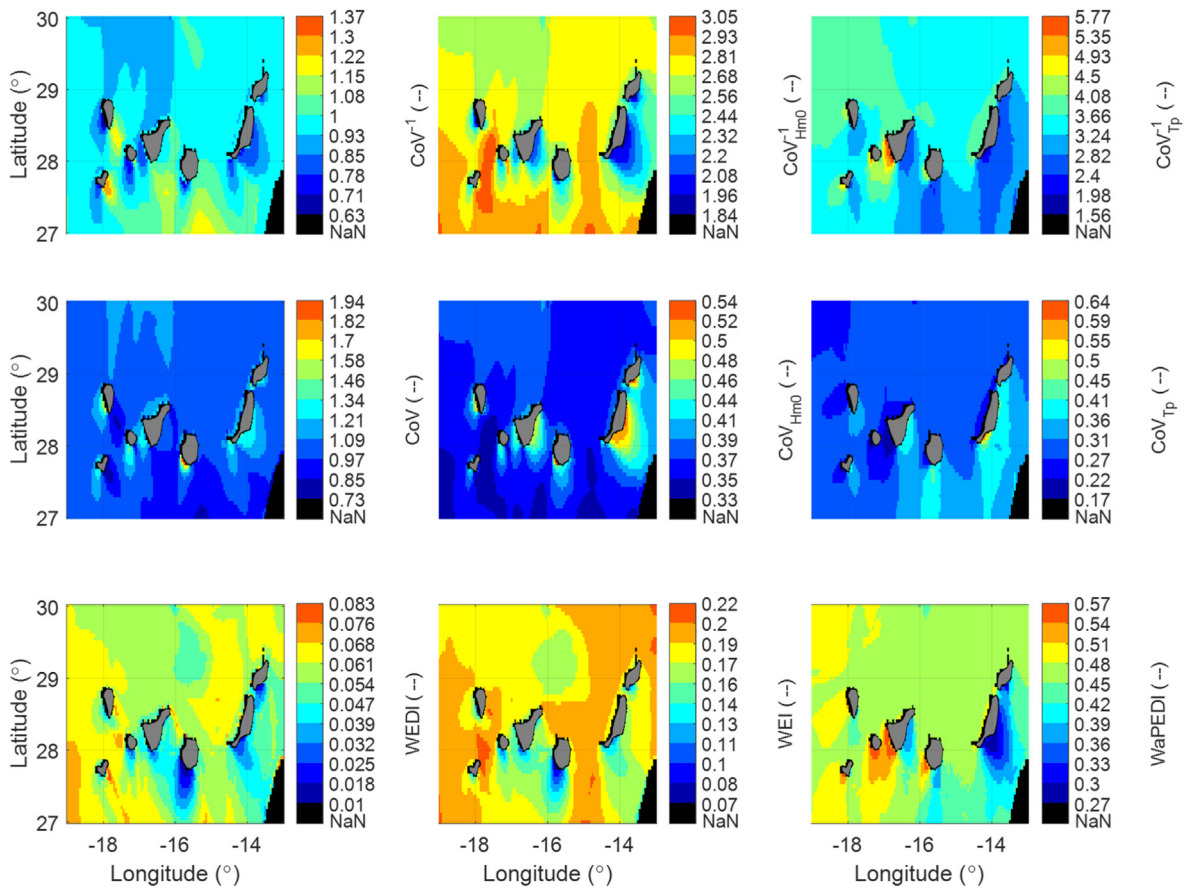


Fig. 6. Inverse of the CoVariance and CoVariance of the wave power (CoV^{-1} and $CoV, -$), significant wave height (CoV^{-1}_{Hm0} and $CoV_{Hm0}, -$), wave peak period (CoV^{-1}_{Tp} and $CoV_{Tp}, -$), Wave Energy Development Index (WEDI, -), Wave Exploitability Index (WEI, -), and Wave Period Exploitation Development Index (WaPEDI). NaN stands for Not-a-Number (from the Copernicus data), and islands are in grey.

AVI, ti, and CoV (and CoV_{Hm0}) maps are similar. However, whereas the annual-, seasonal- and monthly-related aggregated WR-KPIs (Figs. 4 and 5) show only slight variations (mainly southwards: east or west, case-dependent), the three CoVs show high permanent variations in these areas.

Compared to the other WR-KPIs that show more homogeneous results, CoV (as well as AVI and ti) highlights “hotspots”. However, these “hotspots” have low installation potential and renewables are discouraged there (also visible in other locations [37]). This diverges slightly to local sweetspot location-selection (with lower variations) and thus provides relevant information for large-scale/global studies to eliminate regions with high CoVs followed by local analyses of the remaining regions. Its siblings (CoV^{-1}), however, provides more information on the local potential for renewable installation.

The existence of many variations does not necessarily mean that the variations have a large amplitude: WEI, WEDI, and WaPEDI, with similar equations (mean over maximum), highlight where variations may be accentuated and, with their homogenous cartographic resource, are interesting tools for local location-selection. Furthermore, the three indices provide an entirely new visualisation of the resource whilst the main nearshore trends are respected and the confirmation that the north has a more stable resource than in the south.

WEDI and WEI provide quite similar results. Although both are based on entire duration maximums, WEDI uses aggregated annual means (a mix between trend and entire duration analyses), and WEI (and WaPEDI) the mean over the entire duration. However, the

wave period influence (significant in CoV values) is minimal if comparing the spread of CoV/WEDI values with those of CoV_{Hm0} /WEI, while WaPEDI’s behaviour diverges significantly. In summary, the reviewed WR-KPIs thus far can be reduced to SI_p, WEDI and WaPEDI (complementary to wave power and height analyses).

SI_{waveR} (Fig. 7) is the only index that combines wave power flux, height, and period. Its results are similar to those for wave power flux (Fig. 4 and A.3) due to the wave power high weight compared to the wave height and period, as well as a possible consistency of occurrence between the wave height and wave period ranges and those of wave power. Therefore, the information provided by SI_{waveR} is essentially redundant and can be omitted in further location assessment research.

3.1.4. Wave direction

Fig. 8 and Fig. 9 provide the mean wave peak direction ($\theta_{p_m}, ^\circ$) and its validity range (r_p , non-dimensional), respectively, for a) the entire period, b) yearly, c) seasonal, and d) monthly means. The convention is such that North is at 0° (values increasing in the clockwise direction) and the waves are coming from the indicated direction. High r_p values highlight that θ_{p_m} accurately represents a narrow-spread, thereby more suitable for wave farm and wave direction-dependent WECs. Fig. 9 shows large variations northward. This variability is reduced in southern areas (r_p up to 0.96). Although the a)-d) means are similar, and there is consistency between the yearly means, the standard deviation (std) of seasonal and monthly means was as high as $\pm 24^\circ$ in the islands’ south and $\pm 8-16^\circ$ in the region’s western part. That is, in the islands’ south,

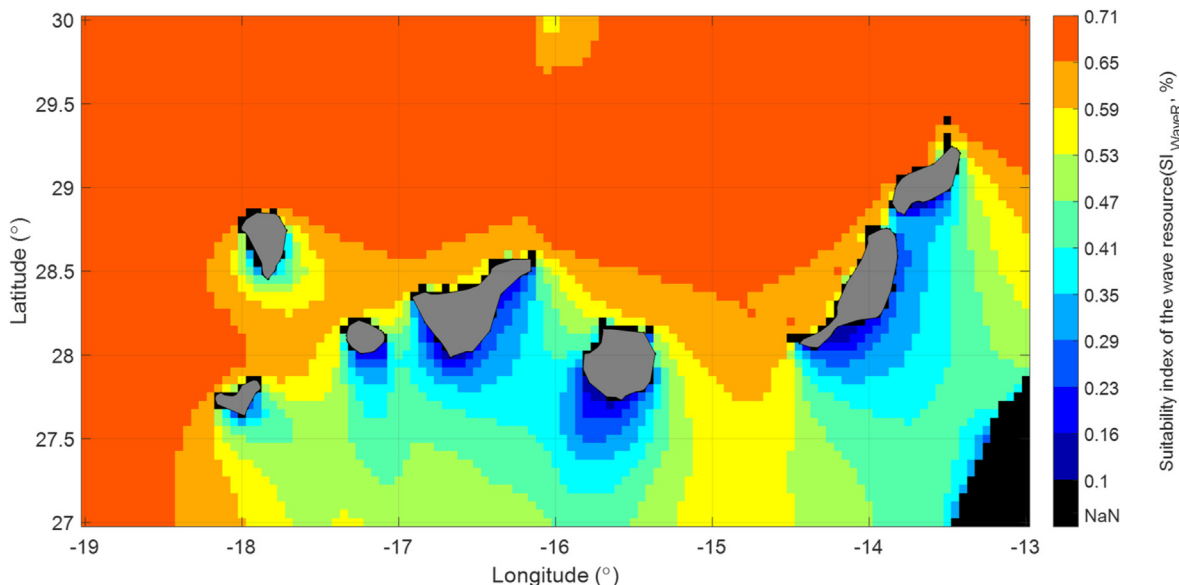


Fig. 7. Suitability Index of the wave resource (SI_{waveR} , %). NaN stands for Not-a-Number (from the Copernicus data) and islands are in grey.

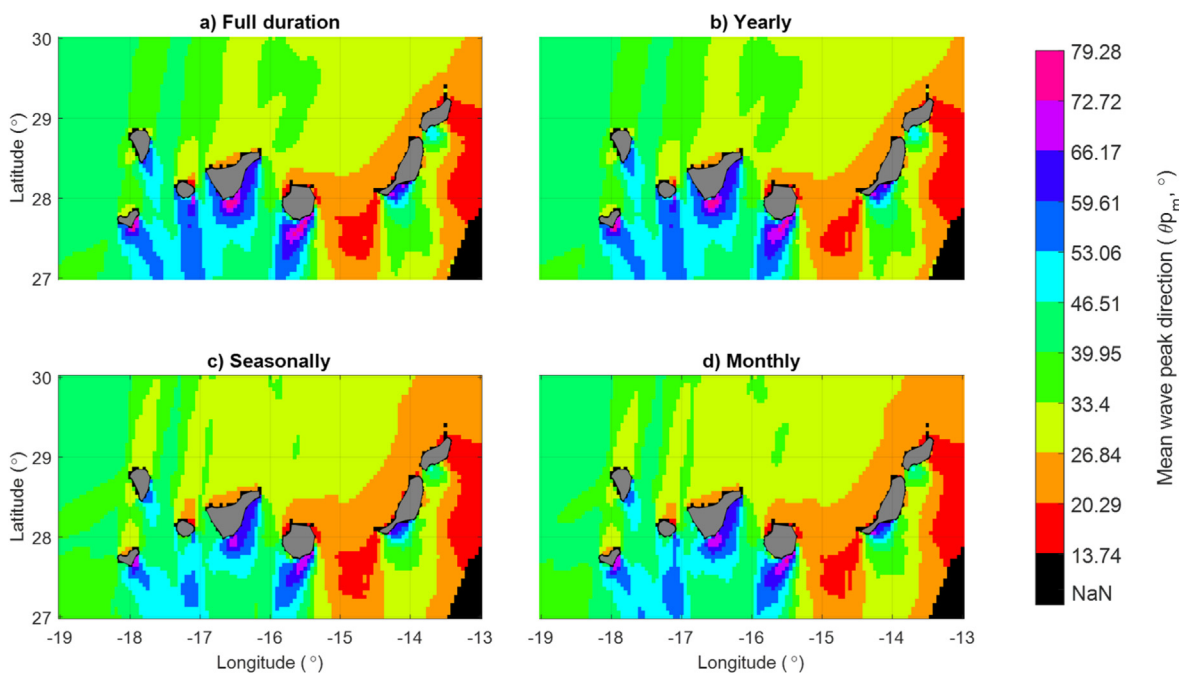


Fig. 8. Mean wave peak direction (θ_{pm} , °). NaN stands for Not-a-Number (from the Copernicus data) and islands are in grey.

θ_{pm} is between 46° further offshore and 79° nearshore. The large seasonal/monthly std of the western islands raises the question of potential seasonality adjustment of a wave farm's installation monthly or instantaneously (e.g. using weathervane moorings). Bozzi et al. [93] showed that farms' q-factor (thereby energy production) is reduced if not properly installed (based on a 30° – almost twice the std found – difference in the directions assessed).

These results somewhat contradict those of SIp (showing best areas to be in the north). Furthermore, θ_{pm} is highly correlated to r_p results, and since r_p informs about the wave direction spread, it should be considered together with SIp. The entire duration (Fig. 9a) is selected as it incorporates both inter- and intra-annual average variations.

3.1.5. Extreme Value Analysis

Fig. 10's left-hand column shows the 30-year return wave height (H_{30}), as in [48], and the right-hand column the 100-year return wave height (H_{100}) [67] (Appendix A provides details regarding EVA). Due to the depth-limited wave breaking, the results are also provided under the rule of thumb (Table A1) [94]. The top and bottom rows are similar due to the large grid size (~ 5 km), avoiding having grid-points in low water depths where EVA wave height overestimations may happen (as reported in [37]).

Although the 30-year approach presents a longer shadow in almost all the islands, between H_{100} and H_{30} , the results are generally proportional. The results' trend does not change with the return period that only affects the ranges of values. Consequently,

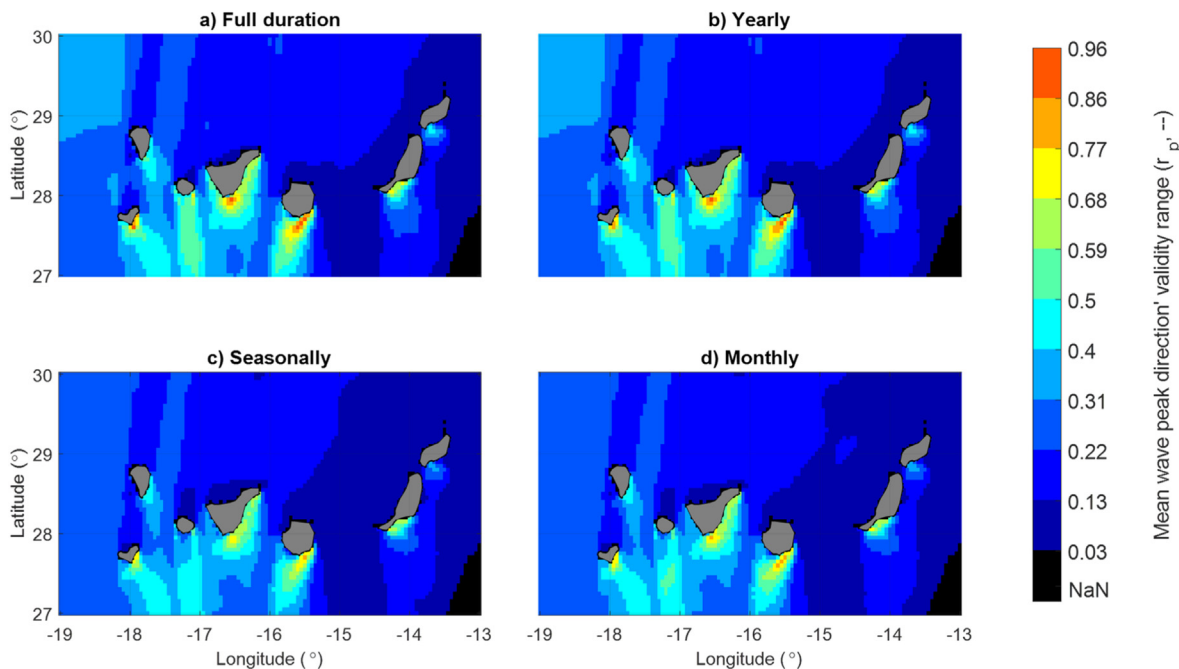


Fig. 9. Range of mean wave peak direction validity ($r_{p, -}$) associated to the values in Fig. 8. NaN stands for Not-a-Number (from the Copernicus data) and islands are in grey.

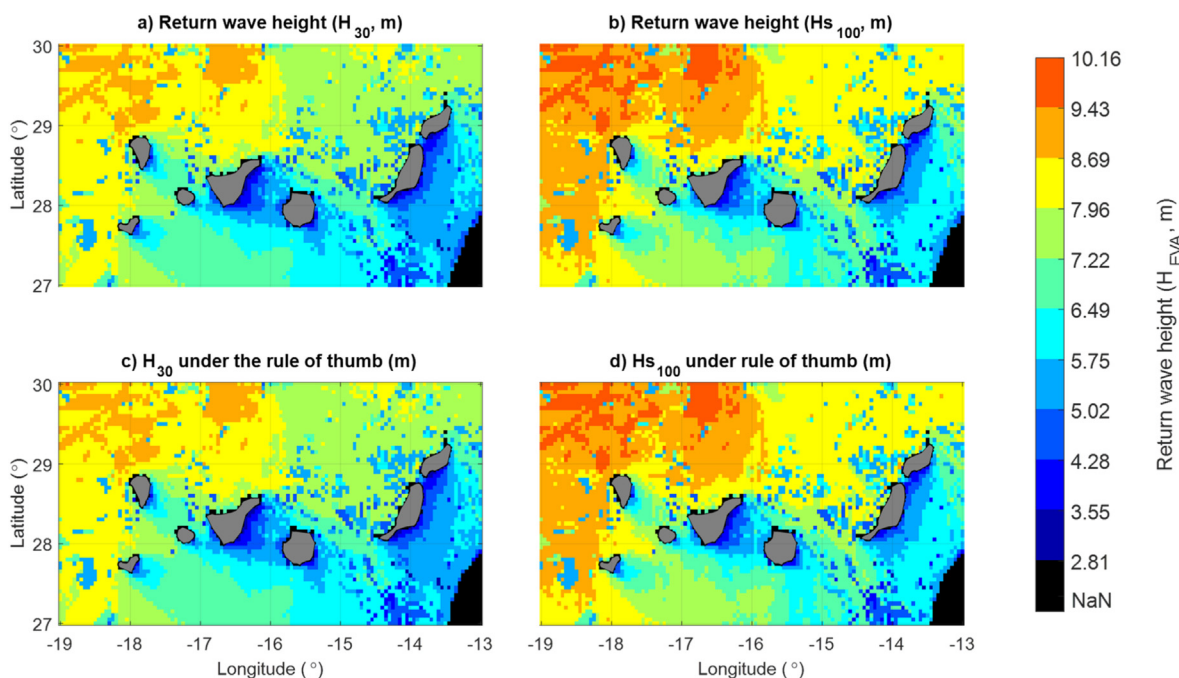


Fig. 10. Return wave height based on Extreme Value Analysis (EVA), with 30- and 100-year return periods, including under the rule of thumb. NaN stands for Not-a-Number (from the Copernicus data) and islands are in grey.

since most H_{EVA} are for periods below or equal to 100 years [67], the analysis of parameters can be reduced to H_{S100} . Overall, in the islands' south and southeast, H_{EVA} is low, meaning that the renewable technologies will not require excessive investment in reinforcement, and commercial devices may not need costly design-adjustments.

3.1.6. Availability and accessibility

Availability and accessibility (Fig. 11) focus on low significant

wave height boundaries. Fig. 11 provides a contrasting analysis: high availability is in the islands' north and west, whereas high accessibility is in the south and east with a 46% average in the north. Accessibility does not need extremely high values, as access to site is needed mainly when WECs require (periodic O&M from once to a few times monthly and occasional emergencies). Therefore, availability has a stronger impact on location selection than accessibility. Consequently, northern regions are the most attractive in this respect.

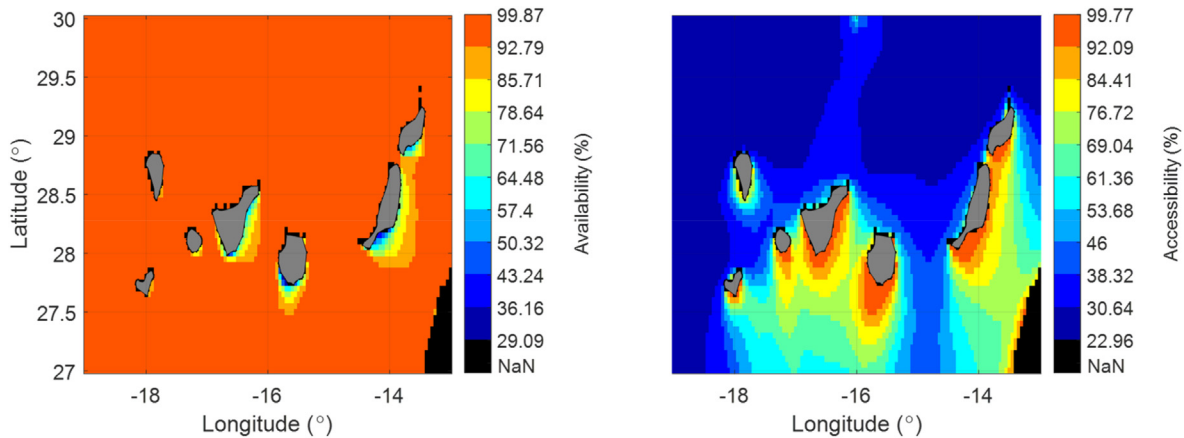


Fig. 11. Availability and Accessibility (both in %) of the Canary Islands' wave power (based on significant wave height analyses). NaN stands for Not-a-Number (from the Copernicus data) and islands are in grey.

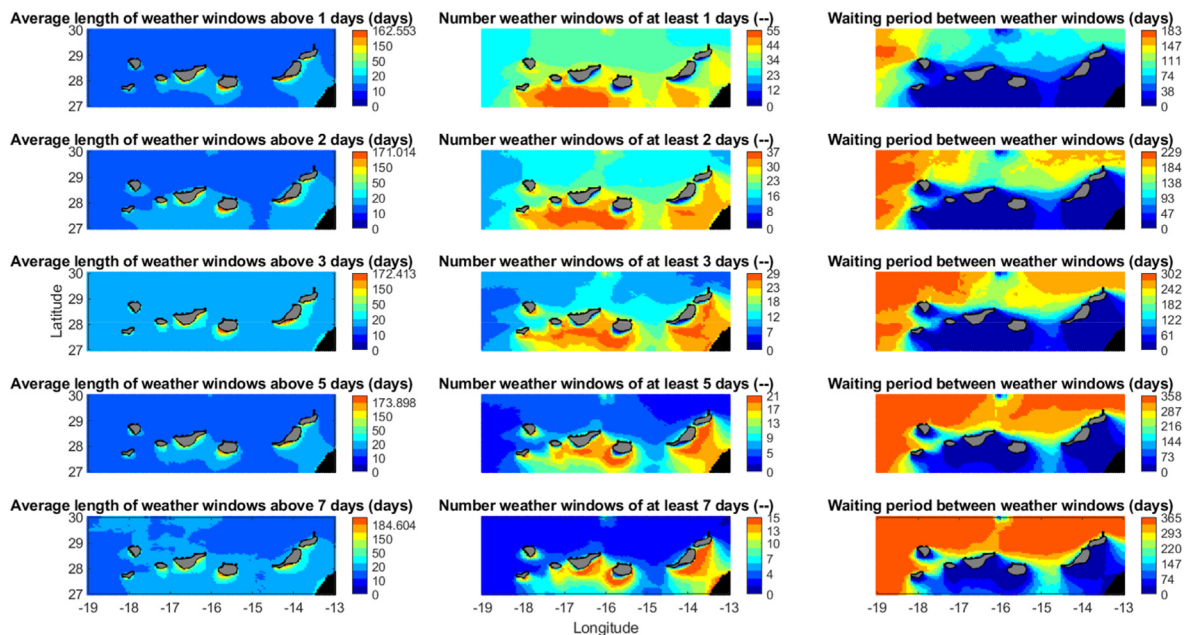


Fig. 12. Annual average length, number of weather windows, and waiting period between them. Black cells are for not-a-number values (from the Copernicus data), and islands are in grey.

Periodical O&M of marine renewable facilities is difficult to achieve due to the variability of wave/weather conditions. Following Section 2.2.3 and [37], Fig. 12 provides the number of weather windows (NWW), their average length (LWW), and waiting period duration (WWP). The islands' WWP ranges from a few days to more than one or two months in northern regions. However, the islands' south nearshore LWW may reach 162 days, thereby reducing their NWW, despite WWPs below a month. Furthermore, for farm installations (and possible overhaul/mid-life refit), the necessary three-days-to-a-week period can be seen in the results. Overall, the average 3-day period of time provides an average in all the weather window aspects. Thus, associated parameters are used to represent this analysis in the rest of the study alongside availability.

3.1.7. Discussion on the integration of the selected wave resource key performance indicators

Idris [95] suggested wave energy densities ≥ 2 kW/m to be considered harvestable, and densities ≥ 20 kW/m rich resources. Global resources are usually assessed on the basis of higher ranges [19,96], however local studies are usually within the first range [81,82,97]. Lavidas and Blok [98] and Portilla et al. [99] highlighted the potential of low energy resources for installation. Annual variability forecasts WEC design needs, while monthly variability informs about energy production [100,101], as shown by the WR-KPIs developed for inter and intra-annual analyses [59,102]. The most important limiting condition is wave height, followed by wave power [15], at the detriment of period and direction. The literature showed that (a) hotspot pre-selection based on wave

power does not represent the direct WEC–location pairing, meaning that not only wave height but also wave period is required, and (b) wave direction is crucial for energy absorption for wave direction-dependent technologies [37] and wave farms [93]. Theories of wave direction assessments [52] have mainly been applied to wind farms [103] and only one parameter introduces the wave period for location-potential assessment (SI_{waveR}). The range, r_p , stands out to assess the wave direction spread (Section 3.1.4) and Section 3.1.3 selects the WEDI and WaPEDI instead of SI_{waveR} . Additionally, the review of the WR-KPIs demonstrates that SIp represents both inter- and intra-annual wave power variations. EVA's Hs_{100} is sufficient due to proportionality between return wave heights (Section 3.2, with rule of thumb disregarded for present irrelevancy). Finally, Section 3.4 demonstrates that availability and the 3-day weather window (number, NWW, average length, LWW, and waiting period, WWP) are sufficient to assess production and O&M feasibilities.

An integration model must be developed using these WR-KPIs to determine the wave resource areas with the highest potential for renewable installations. Ten classes are defined for each index (Table B1, Option 1-b) to reduce their discrepancy in the magnitude of their values. Indeed, the WR-KPIs have very different ranges of values and normalising their ranges will keep this discrepancy in values within 0–1. The classes are defined considering values' range and coverage. Smaller classes' numbers are less important (Appendix B). The weighting offered by the classes might be adjusted in different situations (e.g. long coasts) and project's target (e.g. wave energy focus) especially for variables that are domain-dependent (e.g. SIp). WR-KPIs' classified values were then normalised over the domain and added per grid-cell to provide Fig. 13.a.

Furthermore, Fig. 13.a is virtually the inverse of Fig. 4's P_{year} as the three weather window parameters get the best values for lake-type water-areas, where wave energy is barely harvestable. The higher the NWW and the lower the WWP, the better, but a

full year WWL ensures miserable energy absorption. The classes were accordingly adjusted (Table B1, Option 1-c) to give Fig. 13.b. Choupin et al. [37] also suggested using them only for area filtering, thus Fig. 13.c provides the results without their direct effect, and Fig. 13.d filters the areas for WWL above two months. Restrictions on the other two parameters are integrated in a single class (Appendix B, Table B2), as they cannot be bounded but only rated.

Despite increasing the northern potential, the lake-type areas remain highlighted in Fig. 13.b (adjusted WWL class), which therefore does not help to find high potential marine-areas. Fig. 13.c shows northern areas with potential for farm installation more in line with wave power and SIp (east-west asymmetry), diverging completely from Fig. 13.b and Fig. 13.d. This discrepancy highlights the remaining negative lake-effect of NWW and WWP. For wave power harnessing, SIp should prevail. With a weight of $9-1-3+1$ (9 selected WR-KPIs, minus SIp, minus the three weather window parameters, plus the merged class), following Eq. (16) where SI_{waveR} has a weight of 2 for the two other parameters, SIp would dominate to the detriment of the other WR-KPIs influence (see SI_{waveR} -related discussion, Section 3.1.3). Hence, the weight must be half of this. Considering its own weight and 2 additional WR-KPIs, the weight would be 1.5 obtainable through $1+(2-1)2^{-1}$, and so Fig. 14 shows Fig. 13.d using a $1+(6-1)2^{-1} = 3.5$ weight. In this aspect, multiple variations can be observed, not only affected by the wave period and direction in the south, but also the wave power in the north. The filtering effect of Fig. 13.d) is more visible in Fig. 14, separating islands' low potential areas.

3.2. Part (B): Suitable areas for wave energy production in terms of geographical feasibility

Fig. 15 divides the geographical restrictions into three panels according to Section 2.3.

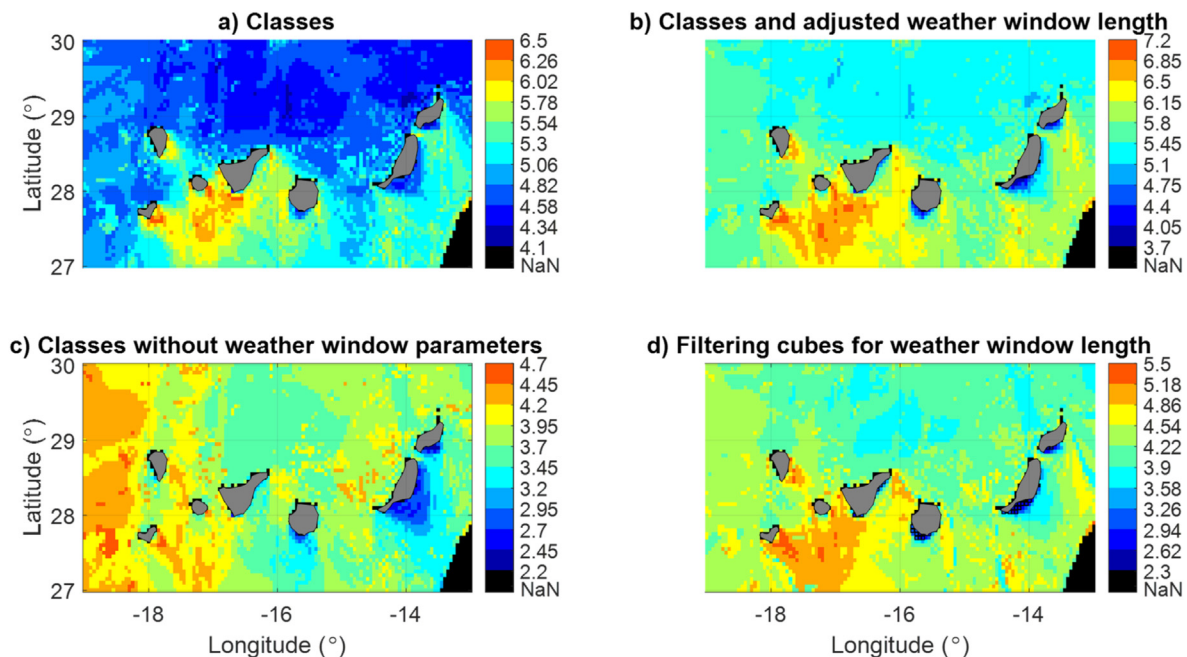


Fig. 13. Potential of wave resource areas for renewable installation based on a) the sum of the classified indices normalised over the domain (non-dimensional), b) same as a) with a different classification of the weather period length (Option 1-c-Table B1), c) same as a) but without the weather window indices, and d) same as a) but number of weather windows and waiting periods merged in one class and with weather window length considered as a filter, for which areas surrounded by black cubes should be disregarded for renewable installations (better visible in Fig. 14). NaN stands for Not-a-Number (from the Copernicus data), and islands are in grey.

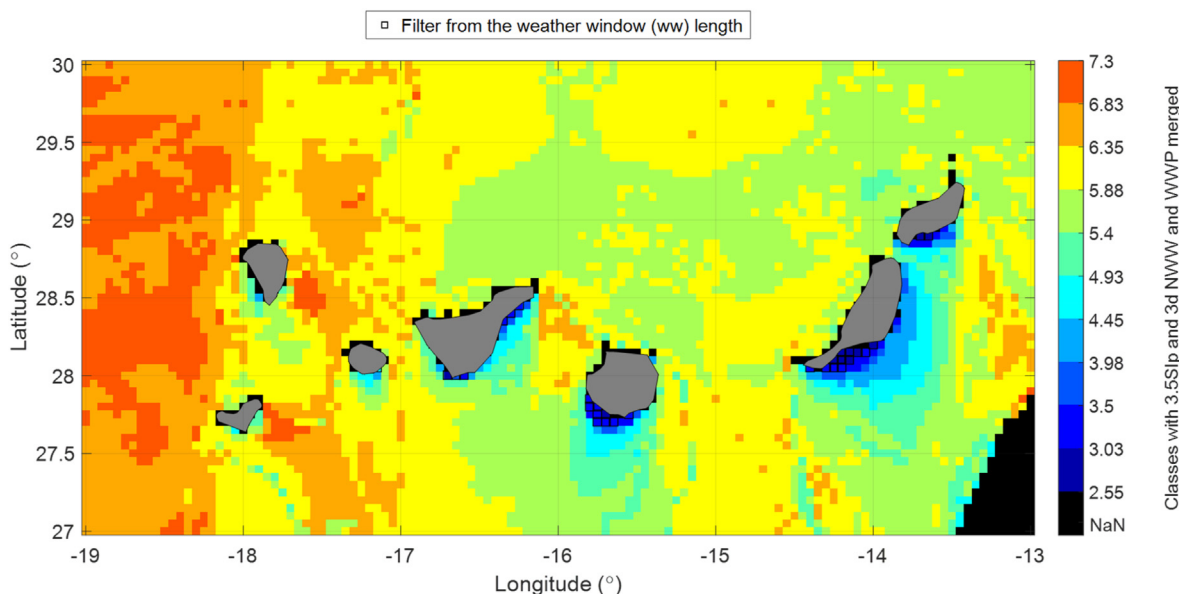


Fig. 14. Results of the normalised classification with a weight of 3.5 to the Suitability Index for wave power flux (Slp), the 3-day (3d) number of weather windows (NWW) and waiting periods (WWP) gathered in a single class, and with filtering of 3d weather window length above 2 months. NaN stands for Not-a-Number (from the Copernicus data), and islands are in grey.

Compiling the geographical restrictions establishes the marine areas where renewable installation is feasible. Fig. 16 shows available areas according to Scenarios 1 and 2 detailed in Table 6: the more conservative Scenario 1 complies with all restrictions, while Scenario 2 reduces their number based on the detailed analyses provided below.

Firstly, aeronautical restrictions related to the manoeuvrability of aircrafts for take-off and landing may not apply since WECs are small compared to wind technologies [104]. The most restrictive environmental laws concern protected areas for bird reproduction and conservation (Fig. 15.a, grey and pink). Despite the scarcity of related studies [105], Grecian et al. [106] confirmed that WECs present a lower risk of collision than wind turbines, especially for underwater fish-feeding birds. A combination of reduced turbulence and decreased grazing pressure may provide favourable conditions for harmful algal bloom formations (light attenuation distorting the food chain in highly populated habitats). However, WECs can encourage damaged flora and fauna habitat recovery by acting as artificial reefs [107]. Low density protected marine fauna/flora areas, with less than five species (Fig. 15.a, red), are removed in Scenario 2.

Sea areas defined as “Important community place in terms of habitats” (Fig. 15.a, dark-green) cover the entire eastern coasts of Lanzarote and Fuerteventura. The corridor formed between the islands and the African coast is a migratory route of cetacean fauna [108]. The size and noise generated by WECs may reduce collisions or confuse these species [109]. However, WEC sounds are similar to pulse noises at frequencies below the hearing capabilities of the vast majority of the marine-fauna [110], avoiding any potential confusion for these species. Hence, nearshore areas are available for WEC installation, although further research is needed to help adjust such restrictions [106,107,110,111].

4. Integration of (A) and (B): Wave resource and installation potential of the canary archipelago

Fig. 17 integrates Fig. 14 where areas are exempt from Scenario 1 (red-line) and Scenario 2 (blue-line) restrictions (black-line for the

maximum installation depth). First, Fig. 17 shows large marine-areas exempt from restrictions. It is best having more good-values (red/orange) in the most restrictive Scenario 1. Most islands have one or more high-potential areas, yet many yellow-middle-potential areas are in Scenario 2. At first sight, La Gomera is the most attractive. Sweet-spot-areas for renewable installation are thus northwest of Gran Canaria and north of Tenerife (all in Scenario 1). Since (a) some classes are fitted to the results (see Appendix B), and (b) Slp, Eq. (13), is normalised over the archipelago-domain, this study’s global reach is slightly limited. Furthermore, as the results are the sum of the classes (Section 3.1.7), the values provide information about the sites’ potential for renewable installation, but do not specify the reason (e.g. higher Slp or higher variability). Hence, the reader is encouraged to refer to the results from the selected WR-KPIs. As high-potential areas are visually easy to detect with the method presented here, this can be an important contribution to guiding the location-selection process, especially because WEC-location pairing based on WEC performance (e.g. Capacity Factor and Energy Demand-Response Index amongst others) often leads to the selection of large areas [37,98]. By giving the exact area-coverage, Table 6 helps determining the number of technologies installable there.

5. Conclusions

This study aims to assess the wave resource potential for renewable installations, especially the WECs (Wave Energy Converters), in the Canary archipelago. A generic method (applicable worldwide) has been developed by: (A) assessing 40 WR-KPIs (Wave Resource Key Performance Indicators) leading to 63 approaches with the aim to reduce this number to the most relevant, complementary, and representative ones; and (B) geographical analyses to determine available areas. Results demonstrated that:

- (A) Inter-annual variations are reduced to Slp (Suitability Index for wave power), which also demonstrated a good representation of intra-annual variations. The introduced WaPEDI (Wave Period Exploitation Development Index) and r_p (mean

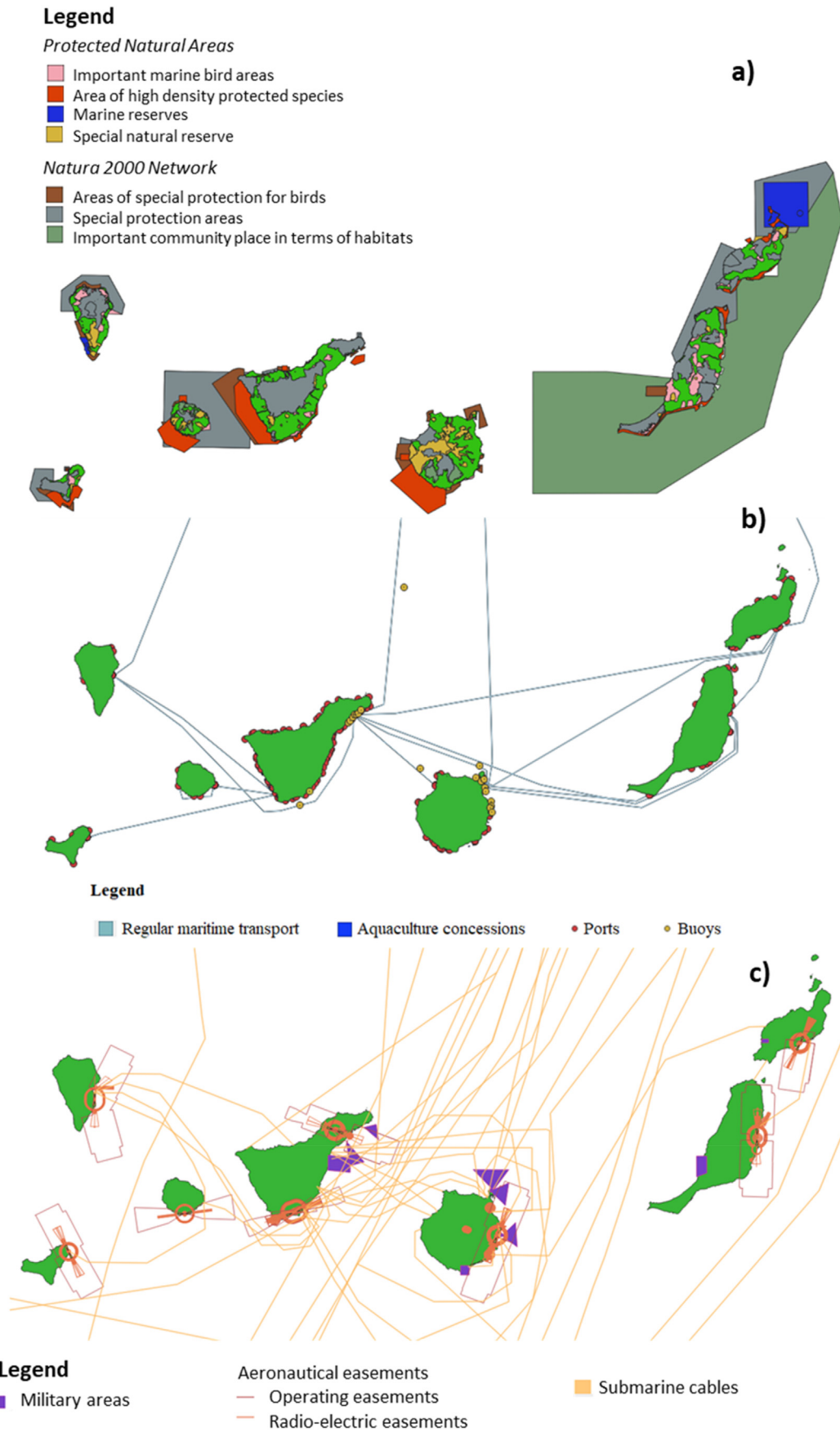


Fig. 15. Marine area restrictions: a) Environmental restrictions; b) Maritime activities, navigation, economic, & technical restrictions; c) Other restrictions.

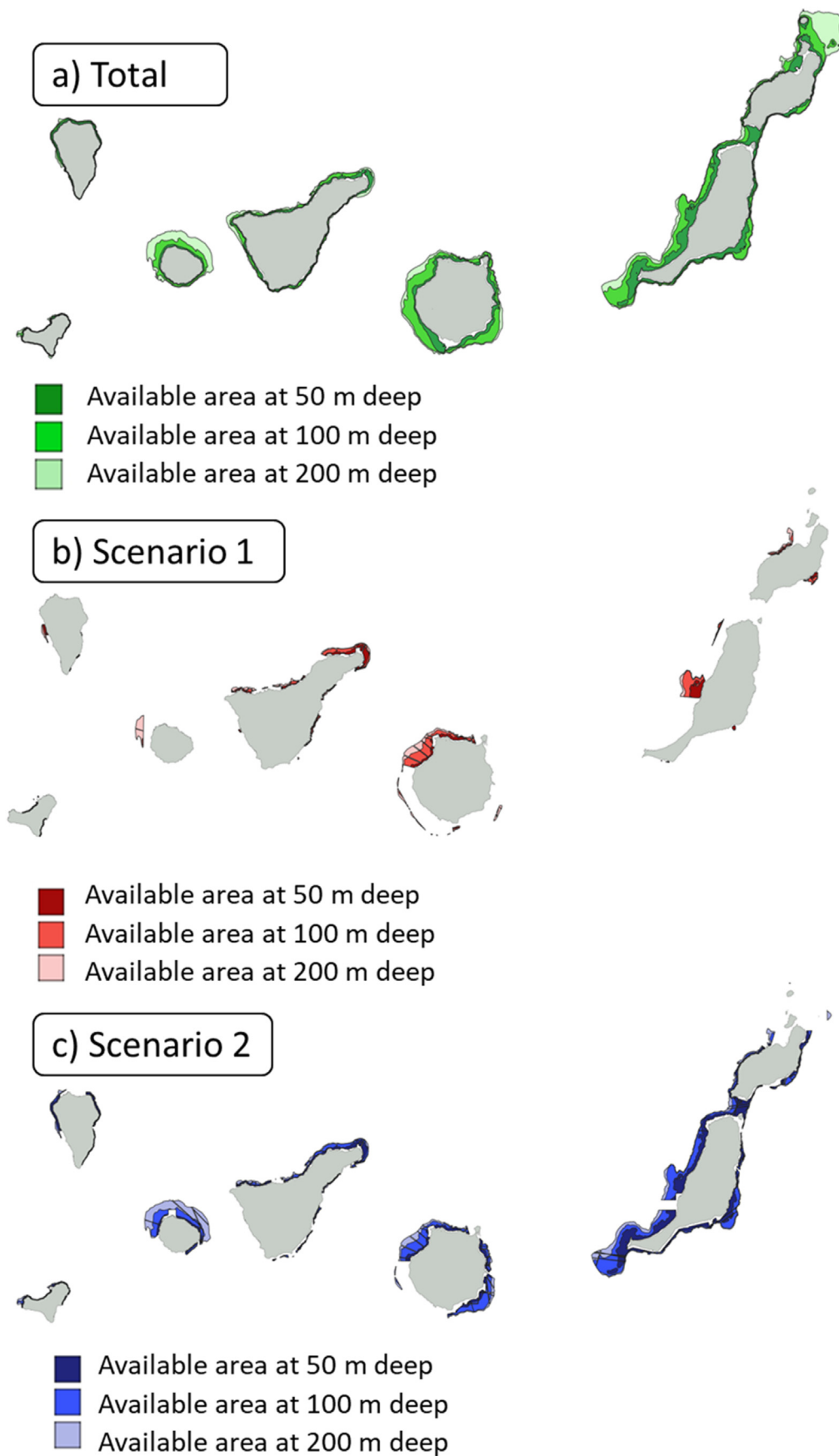


Fig. 16. Available area in the three analysed bathymetric ranges (50, 100, and 200 m). a) Total area of the archipelago below the 200 water depth; b) Area free of restrictions under Scenario 1; c) Area free of restrictions under Scenario 2.

Table 6
Free surface percentage for wave energy production in Scenarios 1 and 2.

Water depth (m)	Islands	Total sea area (km ²)	Area free of restrictions (km ²)	% free area
Scenario 1				
50	Lanzarote & Fuerteventura	843.4	72	8.50%
	Gran Canaria	259.5	44.4	17.10%
	Tenerife	159.7	70.2	41%
	La Gomera	53.7	0	0.00%
	La Palma	53.7	5.6	10.40%
	El Hierro	13.6	2	14.70%
	Canarias	1,383.60	194.2	14.00%
100	Lanzarote & Fuerteventura	1,699.70	172.4	9.80%
	Gran Canaria	792.3	184	23.20%
	Tenerife	291.4	139.4	47.80%
	La Gomera	229.3	2.3	1.00%
	La Palma	91.8	9.9	10.80%
	El Hierro	30.6	4.8	15.70%
	Canarias	3,135.10	512.8	16.40%
200	Lanzarote & Fuerteventura	2,261.30	222.7	10.10%
	Gran Canaria	995.5	286.7	28.80%
	Tenerife	467.8	189.9	40.60%
	La Gomera	520.6	51.5	9.90%
	La Palma	129.1	17.6	13.60%
	El Hierro	60.4	10.4	17.20%
	Canarias	4,434.70	778.8	17.60%
Scenario 2				
50	Lanzarote & Fuerteventura	843.4	603.3	71.50%
	Gran Canaria	259.5	110.4	42.50%
	Tenerife	159.7	91	57.00%
	La Gomera	53.7	32	59.60%
	La Palma	53.7	31.5	58.70%
	El Hierro	13.6	9.2	67.60%
	Canarias	1,383.60	877.4	63.40%
100	Lanzarote & Fuerteventura	1,699.70	1,244.70	73.20%
	Gran Canaria	792.3	396.2	50.00%
	Tenerife	291.4	182.8	62.70%
	La Gomera	229.3	163.7	71.40%
	La Palma	91.8	54.4	59.30%
	El Hierro	30.6	20.5	67.00%
	Canarias	3,135.10	2,062.30	65.80%
200	Lanzarote & Fuerteventura	2,261.30	1,549.10	68.50%
	Gran Canaria	995.5	529.1	53.10%
	Tenerife	467.8	248.4	53.10%
	La Gomera	520.6	419.7	80.60%
	La Palma	129.1	80.4	62.30%
	El Hierro	60.4	40.2	66.60%
	Canarias	4,434.70	2,866.90	64.60%

wave peak direction validity range) were found to be necessary to compensate the lack of wave peak period and direction analyses. Alongside them, the final selected parameters are WEDI (Wave Energy Development Index), Hs₁₀₀ (100-year wave return height assessing the resource harshness based on Extreme Event Analyses), availability (for power absorption), and three weather window O&M-related parameters (length LWW, number NWW, and waiting period WWP) for the 3-day average analysis. The developed integrative model classifies these 9 parameters. Given their alignment, the three weather window parameters together have much influence on the results than the other parameters are individually. This is corrected by merging the NWW and WWP and using LWW as a filter. Similarly, except for SIp, all parameters assess multiple aspects of the resource to the detriment of wave power. Consequently, SIp's weight was increased by a moderated factor of 3.5.

- (B) The geographical overview resulted in the removal of certain restrictions from a Scenario 1, leading to a more flexible Scenario 2.

The model was then integrated with these two scenarios to conclude the main aim of this study. Generally, all the islands have at least one high-potential water area for marine renewable energy installations. On the one hand, Fuerteventura, with high potential in Scenario 2, highlights the need to questioning potential sites' restrictions for WEC installation. On the other hand, La Gomera, with high potential Scenario 1 offshore areas, raises the question of the importance of distance to coastline versus high potential areas. Finally, many sweetspots are located in regions that are not characterised by high wave energy. Hence, high-energetic hotspots are not necessarily the most appealing for wave farm installations opening windows for mild- and low-energetic high-potential areas.

The region assessed in this study (islands with numerous interactions) enabled the different WR-KPIs benchmarking. Yet, in the future, this kind of study should be reproduced over long beach and cliff areas with higher resolution (the present ~5 km lacks nearshore data) to confirm the final WR-KPI-selection. Furthermore, although ROC showed high inter-annual variations leading to the selection of SIp against other metrics (e.g. wave power), the Atlantic Ocean is supposedly characterised by lower inter-annual

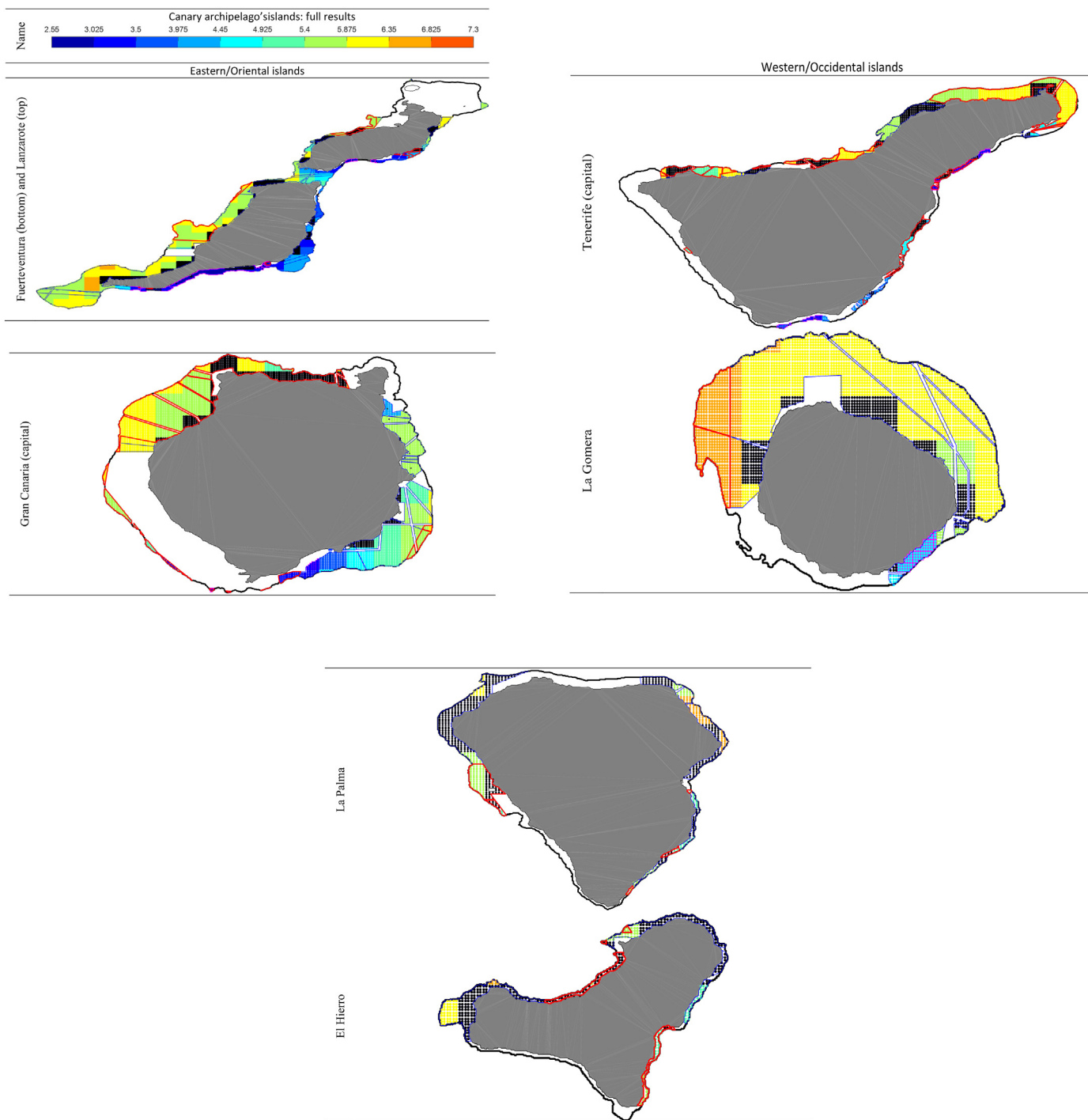


Fig. 17. Zoom of Fig. 14 highlighting the potential for marine installations, especially for WECS, within the non-restricted areas. Scenario 2 is provided with blue lines, Scenario 1 with red, the 200 m depth limit with thick-black lines (see Fig. 16, other bathymetric ranges being omitted for ergonomic reasons). Due to limited grid resolution, original grid-points have been repeated several times within their pixel to fill the non-restricted areas. No interpolation is considered as it distorted the results. Magenta background highlights filtering of weather window length above 2 months (see Fig. 14). NaN stands for Not-a-Number (from the Copernicus data), and islands are in grey.

variations than the Pacific (El Niño and La Niña). Hence, in the future, this study should be reproduced in Pacific locations. Moreover, for other locations, classes/weights adjustments might be required especially regarding the domain-dependent indexes (e.g. S1p), and for project's goals (that might also affect the index selection). Although these results are more applicable to WECs, they can be extended to other renewable energies (e.g. WECs can offer protection for instance to floating solar or offshore wind farms).

CRediT authorship contribution statement

Ophelie Choupin: Conceptualization, Investigation, Methodology, Software, Data curation, Formal analysis, Resources, Validation, Writing – original draft, Writing – review & editing. **B. Del Río-Gamero:** Conceptualization, Resources, Methodology, Data curation, Formal analysis, Investigation, Validation, Visualization, Writing – original draft, Writing – review & editing. **Julieta Schallenberg-Rodríguez:** Project administration, Supervision, Validation, Writing – review & editing. **Pablo Yáñez-Rosales:** Conceptualization, Resources, Methodology, Data curation, Formal analysis, Investigation, Visualization.

Declaration of competing interest

The authors declare that they have no known competing financial interests or personal relationships that could have appeared to influence the work reported in this paper.

Acknowledgements

This research has been co-funded by the ERDF, INTERREG MAC 2014–2020 programme, within the E5DES project (MAC2/1.1a/309). Additionally, some of this research was conducted under Postgraduate Research Scholarships of the first author who would like to acknowledge Griffith University for this support and a great acknowledgment to the Institute of Oceanography of the University of São Paulo and CAPES (Coordenação de Aperfeiçoamento de Pessoal de Nível Superior)/PROEX (Programa de Excelência Acadêmica) for a Doctor of Science research scholarship, Processo: 88887.614992/2021–0, that followed. No funding sources had any influence on study design, collection, analysis, or interpretation of data, manuscript preparation, or the decision to submit for publication. We are also grateful to Rodger Tomlinson, Amir Etemad-Shahidi, Michael Henriksen, and Fernando Pinheiro Andutta for their guidance and advice on the project involving the results of this study, as well as Nicolas Guillou, George Lavidas, Bahareh Kamranzad, and Jose Antonio Carta for their guidance in the application of the indexes and metrics.

Appendix A. Complementary figures to the metric and index analyses

As many results from the literature are based on the deep water equation, Fig. A.1 highlights the difference between the deepwater assumption and the consideration of intermediate and shallow water depths. As found in [41], generally the deepwater slightly underestimates the wave power.

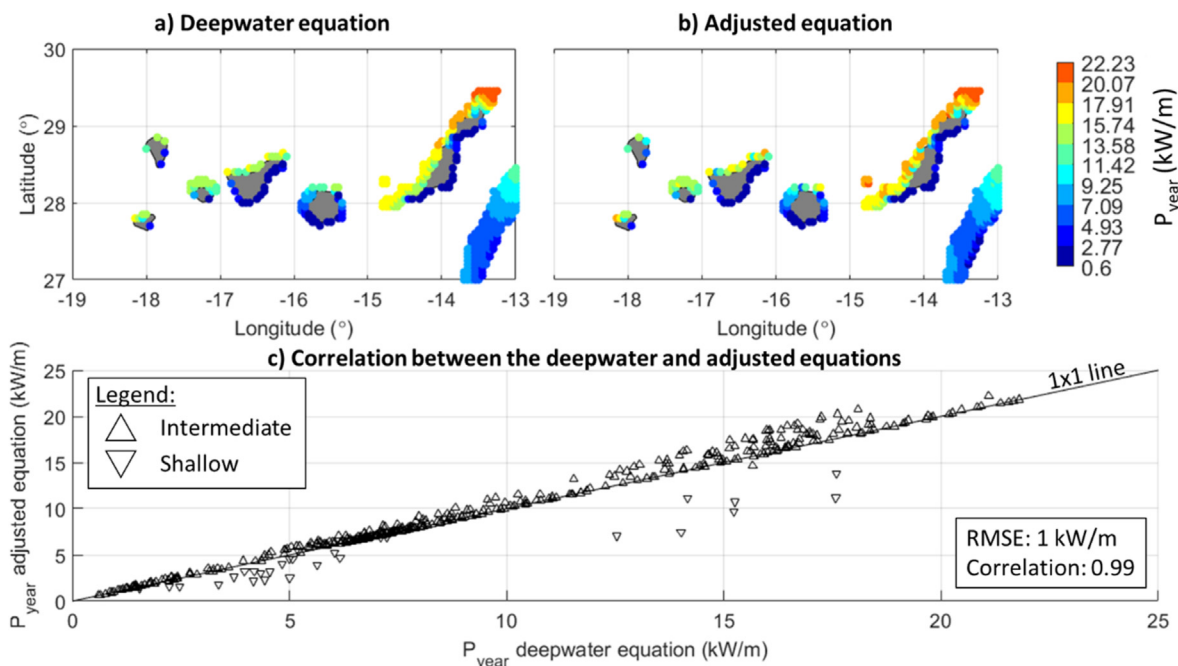


Fig. A.1. Comparison between the 27-year annual mean wave power P_{year} (kW/m) with a) deepwater equations, and b) the adjustment to consider intermediate and shallow water equations when the sea-states are within the corresponding ranges according to Table 1, both for the cells showing at least one non-deepwater sea-state within the 27 years. The legend in c) showing the P_{year} correlation between the selected cells of a) and b) provides the range of water depth for each cell's maximum wave energy period obtained during the 27 years. The Root-Mean-Square-Difference, RMSD (also referred to as the root-mean-square-error), and the correlation [112] between the cells in a) and b) are provided in c).

Table A.1 shows complementary WR-KPIs from the literature. Fig. A.2 provides WR-KPIs related to time and power; Fig. A.3 focuses on different wave energy-based WR-KPIs (including the mean wave power, the normalised available wave power from [113]

is omitted as it would vary following P_{mean} since it is simply divided by the domain's maximum P_{mean}); Fig. A.4 shows complementary EVA parameters.

Table A.1
Complementary Wave Resource Key Performance Indicators.

Concept	Formula		Definition	Expected range of values and objective value
Metrics and indices				
Total hours all year round [t, h] [67]	$t = \text{mean}(\text{number of hours of the years of the duration})^*$	(A.1)	Indicates the mean number of hours in the year. * often $t = 8760$ h	$t \geq 0$ N/A
Theoretical exploitable time [te, h] [67]	$te = J \geq 2 \text{ kW}$	(A.2)	Indicates the potential of hours enabling power harvesting.	$te \geq 0$ High (for lots of power potentially harvestable)
Annual theoretical exploitable time [te _{annual-mean} , h] [67]	$te_{\text{annual-mean}} = \text{mean}(te_{\text{year}})$	(A.3)	Indicates the annual potential of hours enabling power harvesting on average.	$te_{\text{annual-mean}} \geq 0$ High**
Annual mean wave power flux [P _{year} , kW/(year)] [114]	$P_{\text{year}} = \text{mean}(J_{\text{year}})$	(A.4)	Estimates how much power flux is harvestable yearly as the average of the yearly average wave power (J _{year}).	$P_{\text{year}} \geq 0$ High**
Mean wave power [P _{mean} , kW/m] [67]	$P_{\text{mean}} = \text{mean}(J)$	(A.5)	Provides how much power can be absorbed on average over the entire duration.	$P_{\text{mean}} \geq 0$ High**
Exploitable storage of wave energy per unit area [Ee, kWh/m] [67]	$Ee = P_{\text{mean}} te$	(A.6)	Assesses in different stations the possibility of utilizing wave energy converters over the entire duration.	$Ee \geq 0$ High**
Annual total wave energy per unit area [Ee _{full} , kWh/m]	$Ee_{\text{full}} = P_{\text{mean}} te_{\text{year}}$	(A.7)	Assesses the possibility of utilizing wave energy converters over an average year in different stations.	$Ee_{\text{full}} \geq 0$ High**
Total storage of wave energy per unit area [Et, kWh/m] [67]	$Et = P_{\text{mean}} t$	(A.8)	Assesses the availability of the wave energy flux over an average year in different stations.	$Et \geq 0$ High**
Total wave energy [AAE _{total} , kWh/m(/duration)] [59]	$AAE_{\text{total}} = \sum J$	(A.9)	Provides the total energy over the entire duration.	$AAE_{\text{total}} \geq 0$ High**
Mean annual wave energy [E _{year} , kWh/m(/years)]	$E_{\text{year}} = \text{mean}(J_{\text{total year}})$	(A.10)	Is the mean of the total yearly energy (J _{total year}), and so provides how much energy is available in a year, on average.	$E_{\text{year}} \geq 0$ High**
Total wave power variability index [twpvi, kW/m]	$twpvi = \frac{\max(J) - \min(J)}{n}$	(A.11)	With n the number of years, the index (non-defined previously) assesses the maximum range of wave power flux normalised to the duration.	$twpvi \geq 0$ Low (for a relative stability of the resource)
Extreme Event Analysis (EVA) parameters				
EVA's statistical significant wave height - design wave height [H _{1/3-design} , m]	Is the mean of the one-third maximum wave height from the continuous distribution's shape estimated from the POT and i.i.d. (without the need of return wave height).			
EVA's wave height hours to the entire duration [H _{s-ratio} , -]	The coefficient between the entire duration's number of hours, and EVA's number of significant wave heights (after POT and i.i.d) to highlight EVA's pixelisation and the relationship between high wave heights offshore, generally smoothening and lowering this ratio, and smaller waves nearshore with distinguished wave height peaks, leading to a smaller discontinuous EVA distribution and thus higher ratios.			
Return wave height rough estimations [H _{EVA-rough} , m]	Is 1.2 times the maximum wave height.			
Wave height rule of thumb limitation [H _{check} , m] [94]	Is two-third of the water depth, a limitation that waves should not be above.			

**If too high it may reduce the potential for wave energy harvesting.

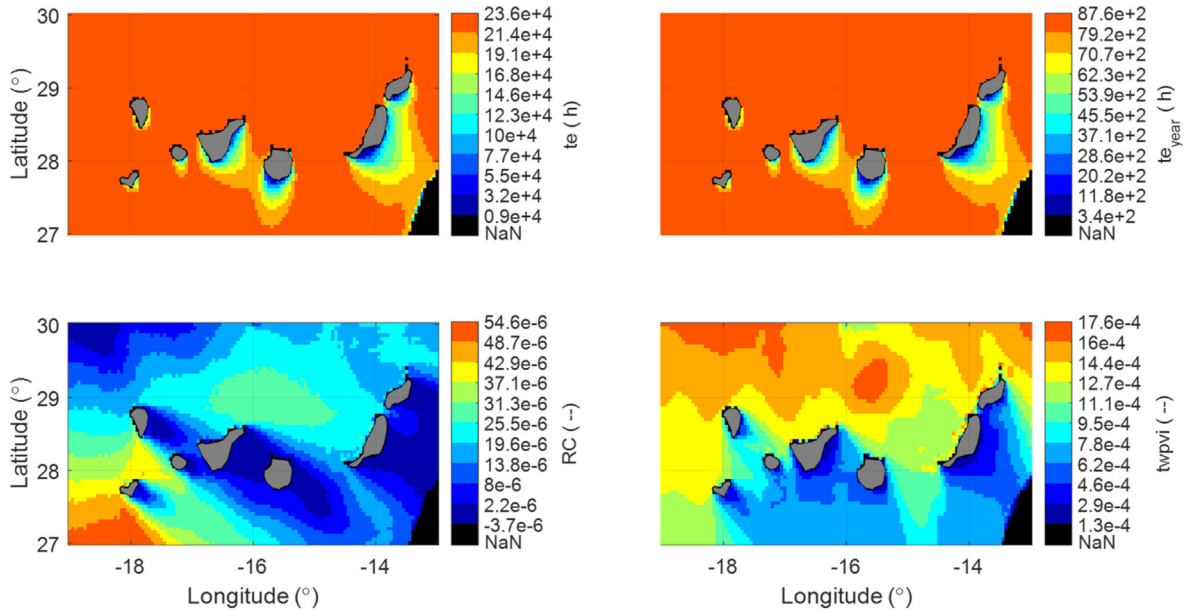


Fig. A.2. Total exploitable time (t_e , h), total annual-mean exploitable time ($t_{e_{year}}$, h), wave power flux Rate of Change over the entire period (RC, -), power variability index estimated for the entire period referred to as the total wave power variability index ($twpvi$, -). NaN stands for Not-a-Number (from the Copernicus data), and islands are in grey.

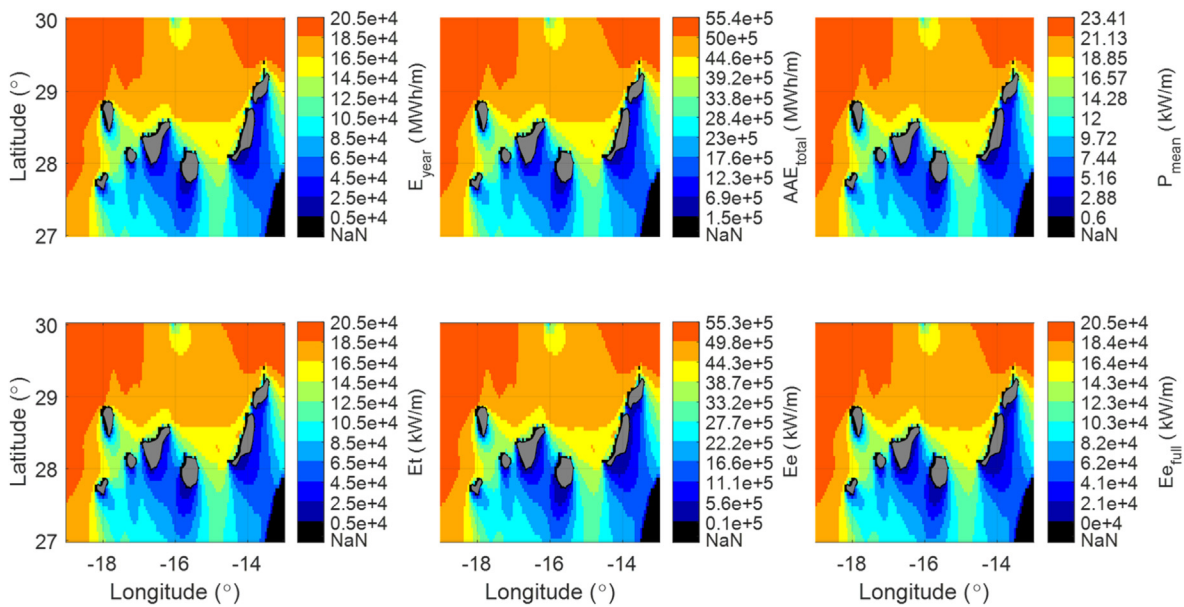


Fig. A.3. Wave energy and power flux analyses with E_{year} (MWh/m) the mean annual wave energy, AAE_{total} (MWh/m), the total wave energy flux production, P_{mean} (kW/m) the total mean of the wave power flux over the entire duration, E_t (kW/m) the total storage of wave energy per unit area, E_e (kW/m) the exploitable storage of wave energy per unit area, and $E_{e_{full}}$ the annual total wave energy per unit area. NaN stands for Not-a-Number (from the Copernicus data), and islands are in grey.

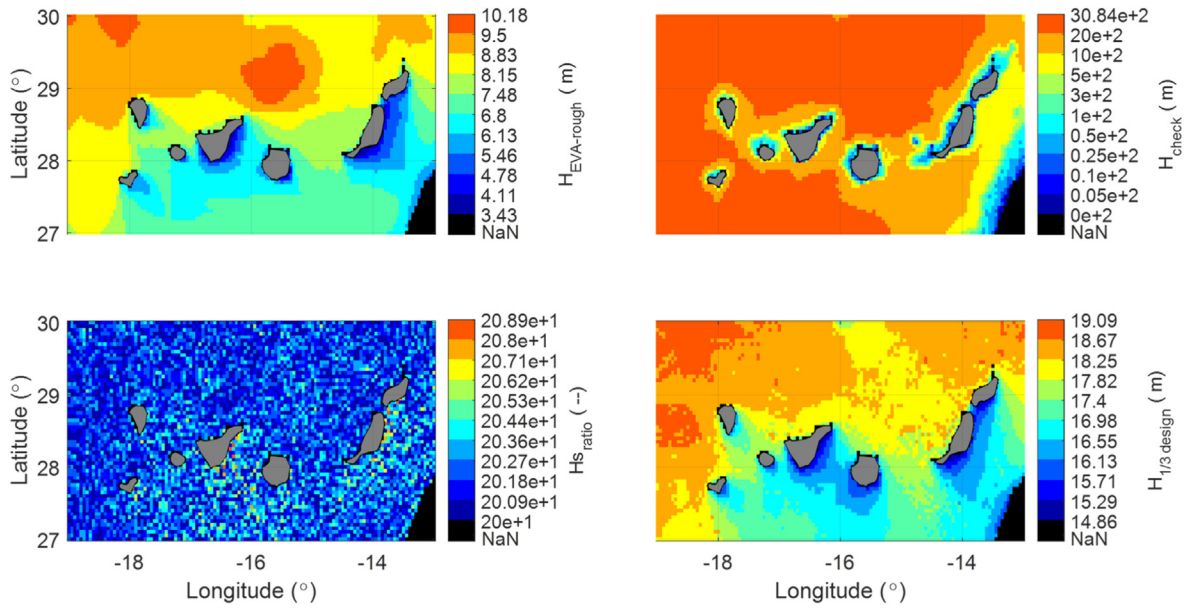


Fig. A.4. Extreme Value Analysis (EVA) complementary parameters: $H_{EVA-rough}$ (m) rough estimation of the return wave height, H_{check} (–) maximum wave height under the rule of thumb, Hs_{ratio} (–) ratio of $H_{EVA-distribution}$ length to total $Hs_{distribution}$ length, and $H_{1/3 design}$ (m), literally, the statistically significant wave height of the $H_{EVA-distribution}$. NaN stands for Not-a-Number (from the Copernicus data), and islands are in grey.

Appendix B: Classification of the resource

The two methods presented in Section 3.1.7 (Table B.1, Option 1-b-c) are based on Option 1-a. It classifies each WR-KPI in ranges that fit the data spread, but as the number of defined classes provides more weight to some parameters, whereas the weighting should be uniform, the number of classes per WR-KPI is normalised to ten ranges in Option 1-b-c. Option 1-c provides the final adjustments (see Section

3.1.7), and Fig. B.1 shows the classified results. An additional quotient-based approach (Fig. B.2) was considered by normalising the WR-KPIs (against the domain's maximums), and dividing the product of those that need to be high by the product of those that need to be low (Table B.1, last-column). Since (a) this approach's highest potential area for renewable installation follows Fig. 14, and (b) it lacks details, it is not presented in Section 3.1.7.

Table B.1

Classification approaches and ranges for the indices, such that Class X: A:B, where X is the level of importance of the class (the higher the better), A and B are the low and high boundaries, respectively, and values belonging to Class X are above or equal to A and strictly below B.

Selected parameters	Option 1-a Ranges of real values and associated class	Option 1-b Normalised ranges	Option 1-c Enhanced ranges
Wave Energy Development Index (WEDI, non-dimensional) needs to be high and hence has an increasing values classification.	Class 1: 0:0.04 Class 2: 0.04:0.054 Class 3: 0.054:0.061 Class 4: 0.061:0.069 Class 5: 0.069:0.083	Class 1: 0.011:0.018 Class 2: 0.018:0.026 Class 3: 0.026:0.033 Class 4: 0.033:0.040 Class 5: 0.040:0.047 Class 6: 0.047:0.054 Class 7: 0.054:0.061 Class 8: 0.061:0.069 Class 9: 0.069:0.076 Class 10: 0.076:0.083	Same as Option 1-b
Wave Period Exploitation Development Index (WaPEDI, non-dimensional) needs to be high and hence has an increasing values classification.	Class 1: 0.27:0.36 Class 2: 0.36:0.42 Class 3: 0.42:0.45 Class 4: 0.45:0.48 Class 5: 0.48:0.51 Class 6: 0.51:0.57	Class 1: 0.27:0.30 Class 2: 0.30:0.33 Class 3: 0.33:0.36 Class 4: 0.36:0.39 Class 5: 0.39:0.42 Class 6: 0.42:0.45 Class 7: 0.45:0.48 Class 8: 0.48:0.51 Class 9: 0.51:0.54 Class 10: 0.54:0.57	Same as Option 1-b
Range of mean wave direction variation validity (r_p , non-dimensional) needs to be high and hence has an increasing values classification.	Class 1: 0.04:0.13 Class 2: 0.13:0.22 Class 3: 0.22:0.4 Class 4: 0.4:0.68 Class 5: 0.68:0.77 Class 6: 0.77:0.96	Class 1: 0:0.1 Class 2: 0.1:0.2 Class 3: 0.2:0.3 Class 4: 0.3:0.4 Class 5: 0.4:0.5 Class 6: 0.5:0.6 Class 7: 0.6:0.7 Class 8: 0.7:0.8 Class 9: 0.8:0.9 Class 10: 0.9:1	Same as Option 1-b

Table B.1 (continued)

Selected parameters	Option 1-a Ranges of real values and associated class	Option 1-b Normalised ranges	Option 1-c Enhanced ranges
Suitability Index for wave power (Slp, non-dimensional) needs to be high and hence has an increasing values classification.	Class 1: 0.03:0.18 Class 2: 0.18:0.33 Class 3: 0.33:0.4 Class 4: 0.4:0.47 Class 5: 0.47:0.55 Class 6: 0.55:0.62 Class 7: 0.62:0.77	Class 1: 0.03:0.11 Class 2: 0.11:0.18 Class 3: 0.18:0.25 Class 4: 0.25:0.33 Class 5: 0.33:0.40 Class 6: 0.40:0.47 Class 7: 0.47:0.55 Class 8: 0.55:0.62 Class 9: 0.62:0.69 Class 10: 0.69:0.77	Same as Option 1-b
Wave return height for a 100-year return period (H_{s100} , m) needs to be low and hence has a decreasing values classification.	Class 1: 10.16:9.43 Class 2: 9.43:8.69 Class 3: 8.69:7.96 Class 4: 7.96:6.49 Class 5: 6.49:5.02 Class 6: 5.02:3.55 Class 7: 3.55:2.81	Class 1: 11:10.2 Class 2: 10.2:9.4 Class 3: 9.4:8.6 Class 4: 8.6:7.8 Class 5: 7.8:7 Class 6: 7:6.2 Class 7: 6.2:5.4 Class 8: 5.4: 4.6 Class 9: 4.6: 3.8 Class 10: 3.8:3	Same as Option 1-b
Availability (in %) needs to be high and hence has an increasing values classification.	Class 1: 0:10 Class 2: 10:20 Class 3: 20:30 Class 4: 30:40 Class 5: 40:50 Class 6: 50:60 Class 7: 60:70 Class 8: 70:80 Class 9: 80:90 Class 10: 90:100	Class 1: 0:10 Class 2: 10:20 Class 3: 20:30 Class 4: 30:40 Class 5: 40:50 Class 6: 50:60 Class 7: 60:70 Class 8: 70:80 Class 9: 80:90 Class 10: 90:100	Same as Option 1-b
3-day number of weather windows (non-dimensional) needs to be high and hence has an increasing values classification. It should be noted that here one weather window is at least 3 days.	Class 1: 0:5 Class 2: 5:10 Class 3: 10:15 Class 4: 15:20 Class 5: 20:25 Class 6: 25:30	Class 1: 0:5 Class 2: 5:10 -> up to minimum one month Class 3: 10:12 Class 4: 12:15 Class 5: 15:18 Class 6: 18:20 -> up to minimum two months Class 7: 20:22 Class 8: 22:25 Class 9: 25:28 Class 10: 28:30 -> up to minimum three months	Same as Option 1-b
3-day weather window average length (in days) needs originally to be high and hence has an increasing values classification in both first column, and the approach of Option 1-c is discussed in Section 3.1.7. It should be noted that here that the minimum window's length is of 3 days.	Class 1: 0:3 Class 2: 3:5 Class 3: 5:7 -> up to one week Class 4: 7:10 Class 5: 10:14 -> up to two weeks Class 6: 14:30 -> up to one month Class 7: 30:60 -> up to two months Class 8: 60:90 -> up to three months Class 9: 90:110 -> up to four months Class 10: 110:150 -> up to five months Class 11: 150:180 -> up to six months	Class 1: 0:3 Class 2: 3:5 Class 3: 5:10 Class 4: 10:14 -> up to two weeks Class 5: 14:30 -> up to one month Class 6: 30:60 -> up to two months Class 7: 60:90 -> up to three months Class 8: 90:110 -> up to four months Class 9: 110:150 -> up to five months Class 10: 150:180 -> up to six months	Class 6: 0:3 Class 9: 3:5 Class 10: 5:10 Class 8: 10:14 -> up to two weeks Class 7: 14:30 -> up to one month Class 5: 30:60 -> up to two months Class 4: 60:90 -> up to three months Class 3: 90:110 -> up to four months Class 2: 110:150 -> up to five months Class 1: 150:180 -> up to six months
3-day weather window average waiting period between them (in days)	Class 1: 365:180 Class 2: 180:120 Class 3: 120:60 Class 4: 60:30 Class 5: 30:20 Class 6: 20:15 Class 7: 15:10 Class 8: 10:5 Class 9: 5:0	Class 1: 365:274 Class 2: 274:180 Class 3: 180:120 Class 4: 120:60 Class 5: 60:30 Class 6: 30:20 Class 7: 20:15 Class 8: 15:10 Class 9: 10:5 Class 10: 5:0	Same as Option 1-b

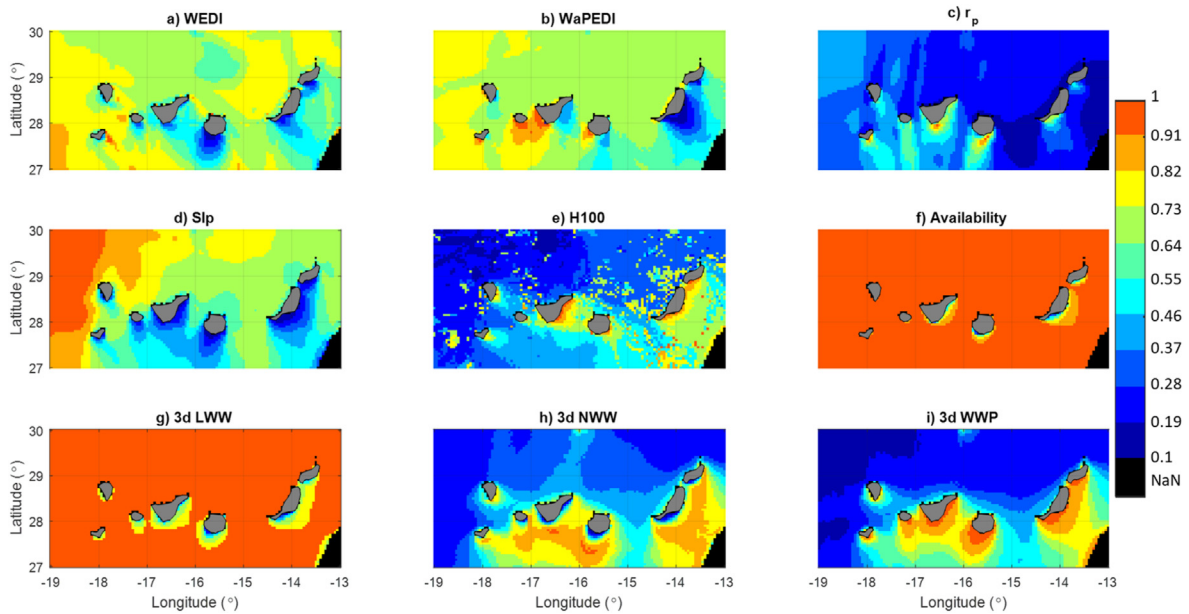


Fig. B.1. Values of the selected Wave Resource Key Performance Indicators under the classification and normalisation over the domain and thereby non-dimensional. From top to bottom and left to right: Wave Energy Development Index (WEDI), Wave Period Exploitation Development Index (WaPEDI), range of validity of the mean wave direction (r_p), Sustainability index for the wave power (Slp), wave return Height for a 100-year return period (H_{100}), availability, 3-day Weather Window Length (3d LWW), Number of Weather Windows of at least 3 days (3d NWW), and Waiting Period between these Weather Windows (3d WWP).

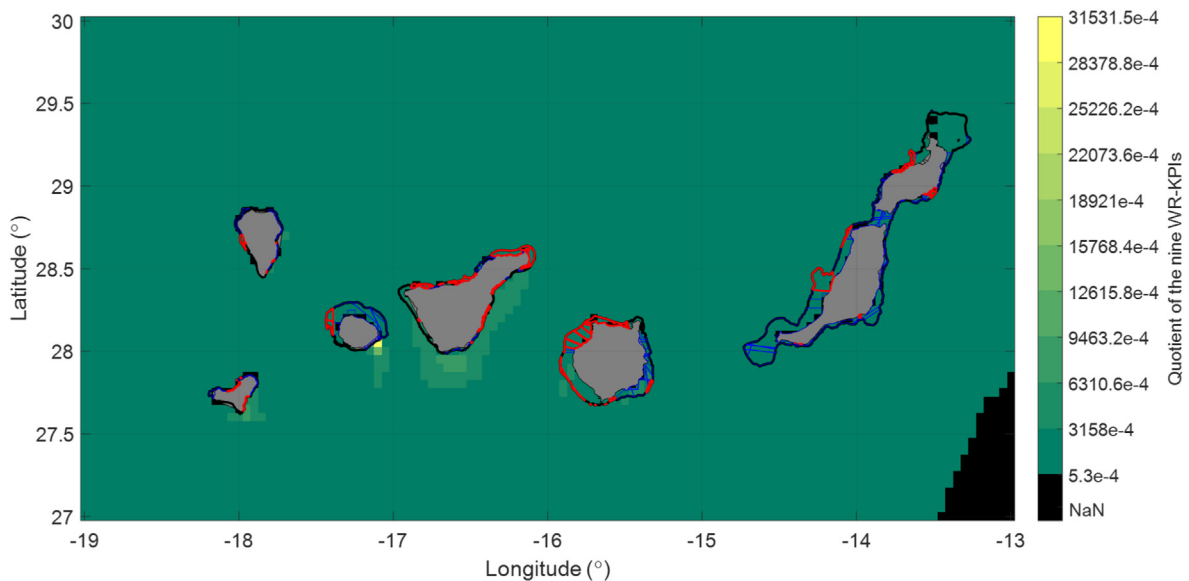


Fig. B.2. Distribution of the quotient of the nine Wave Resource Key Performance Indicators selected for wave resource for potential assessment of marine areas for renewable installation (Section 3.1). Scenario 2 is highlighted in blue lines, red for Scenario 1, and black for the 200 m depth limit. NaN stands for Not-a-Number (from the Copernicus data), and islands are in grey.

Table B.2 shows the merging of NWW and WWP mentioned in Section 3.1.7 and displayed in Figure B.4. Assuming a 150-unit offshore wind farm, two maintenances per turbine per year and that each maintenance takes between 12 and 18 h [115], the average total O&M length is $(2 \times 14 \times 150^{-24})^{-30} \approx 6$ months. Assuming that a wave farm has fewer units for about four times

more O&M [116,117] those numbers can apply. Table B.2's best class (Class 10) is explained by considering a 2-month filtering WWL and that the 3-day NWW can reach 30 (3-month total). The other combinations are based on Fig. B.3 and ensuring continuity between the classes.

Table B.2

Distribution of the quotient approach for wave resource for the assessment of the potential of a marine area for renewable installation.

	Number of weather windows [Original 1-b class(es) range]	Waiting periods [Original 1-b class(es) range]
Class 1	0:10 [Class 1–2]	365:274 [Class 1]
Class 2	0:10 [Class 1–2]	274:180 [Class 2]
Class 3	10:15 [Class 3–4]	274:180 [Class 2]
Class 4	10:15 [Class 3–4]	60:180 [Class 3–4]
Class 5	15:20 [Class 5–6]	60:180 [Class 3–4]
Class 6	10:15 [Class 3–4]	0:60 [Class 5–10]
Class 7	15:20 [Class 5–6]	30:60 [Class 5]
Class 8	15:20 [Class 5–6]	0:30 [Class 6–10]
Class 9	20:30 [Class 7–10]	14:30 [Class 6–7]
Class 10	20:30 [Class 7–10]	0:14 [Class 8–10]

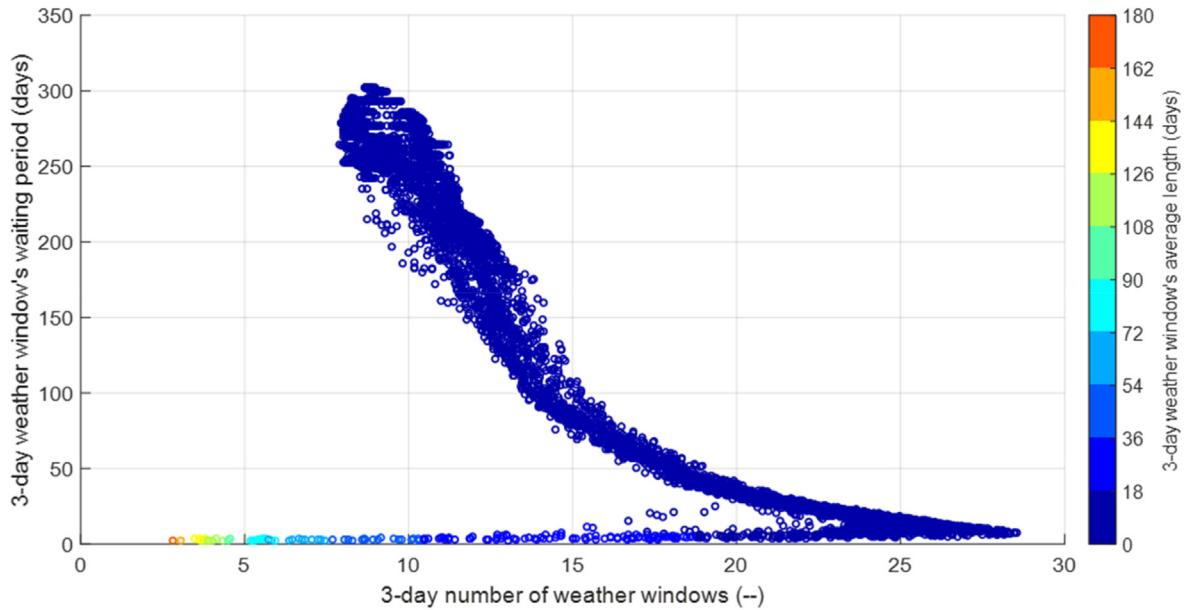


Fig. B.3. Correlation between the three weather window parameters.

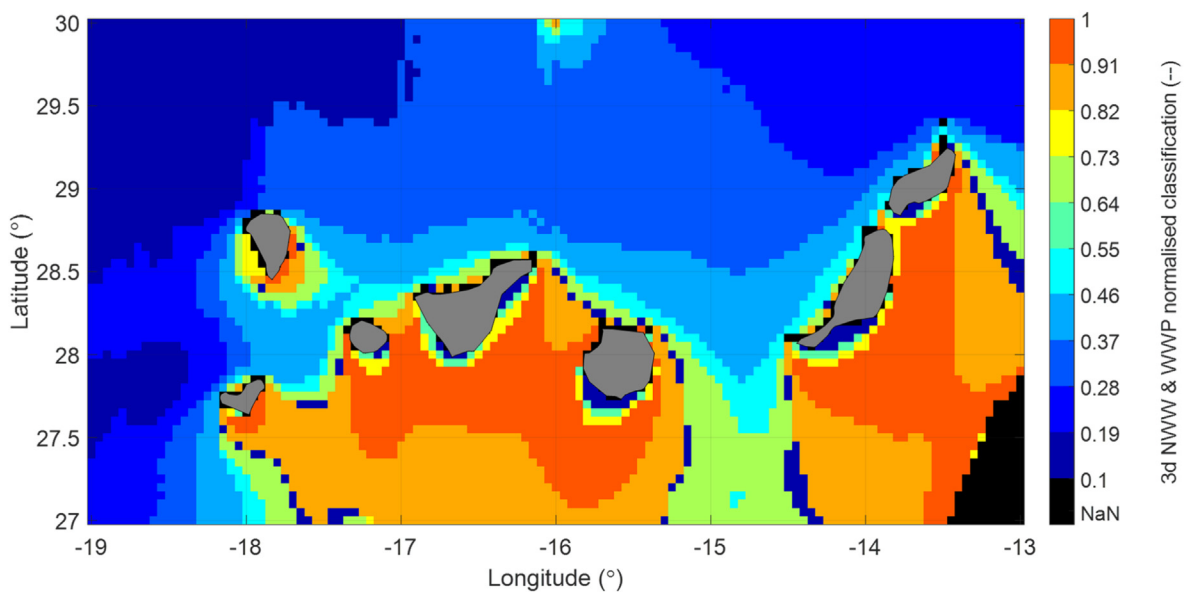


Fig. B.4. Merged classification (normalised over the entire domain and thereby non-dimensional) of the Number of Weather Windows of at least 3 days and the Waiting Period between them (3d NWW and WWP, respectively). NaN stands for Not-a-Number (from the Copernicus data), and islands are in grey.

References

- [1] S. Stevović, D. Golubović, S. Mirjanić, Renewable Energy Sources and Correlated Environmental Systems, 2020, pp. 530–540, https://doi.org/10.1007/978-3-030-18072-0_61.
- [2] D.S. Ryberg, Z. Tulemat, D. Stolten, M. Robinius, Uniformly constrained land eligibility for onshore European wind power, *Renew. Energy* 146 (2020) 921–931, <https://doi.org/10.1016/j.renene.2019.06.127>.
- [3] C. Müller, A. Hoffrichter, L. Wyrwoll, C. Schmitt, M. Trageser, T. Kulms, D. Beulertz, M. Metzger, M. Duckheim, M. Huber, M. Küppers, D. Most, S. Paulus, H.J. Heger, A. Schnettler, Modeling framework for planning and operation of multi-modal energy systems in the case of Germany, *Appl. Energy* 250 (2019) 1132–1146, <https://doi.org/10.1016/j.apenergy.2019.05.094>.
- [4] T. Pennock, S. Delahaye, System benefits from integration of marine renewables, in: *Proceedings of the International Conference on Ocean Energy 2021 (ICOE2021)*, Virtual Conference Hosted by USA, 2021.
- [5] J. Schallenberg-Rodríguez, Julieta, Del Río-Gamero, Beatriz, Noemi Melián-Martel, Lis Alecio, Tyrone, Gonzalez-Herrera, Energy supply of a big size desalination plant using wave energy. Practical case: north of gran Canaria, *Appl. Energy* 278 (2020) 115681.
- [6] A. Pecher, J.P. Kofoed, Handbook of Ocean Wave Energy, 2017, <https://doi.org/10.1007/978-3-319-39889-1>.
- [7] S. Astariz, C. Perez-Collazo, J. Abanades, G. Iglesias, Towards the optimal design of a co-located wind-wave farm, *Energy* 84 (2015) 15–24, <https://doi.org/10.1016/j.energy.2015.01.114>.
- [8] S. Astariz, C. Perez-Collazo, J. Abanades, G. Iglesias, Co-located wave-wind farms: economic assessment as a function of layout, *Renew. Energy* 83 (2015) 837–849, <https://doi.org/10.1016/j.renene.2015.05.028>.
- [9] H.C. Gils, S. Simon, Carbon neutral archipelago – 100% renewable energy supply for the Canary Islands, *Appl. Energy* 188 (2017) 342–355, <https://doi.org/10.1016/j.apenergy.2016.12.023>.
- [10] J. Fernández Chozas, Energía Unidmotriz, Una aproximación al aprovechamiento de la energía de las olas para la generación de electricidad, Editorial, 2012.
- [11] R.A. Arinaga, K.F. Cheung, Atlas of global wave energy from 10 years of reanalysis and hindcast data, *Renew. Energy* 39 (2012) 49–64, <https://doi.org/10.1016/j.renene.2011.06.039>.
- [12] Y. Lin, S. Dong, Wave energy assessment based on trivariate distribution of significant wave height, mean period and direction, *Appl. Ocean Res.* 87 (2019) 47–63, <https://doi.org/10.1016/j.apor.2019.03.017>.
- [13] E. Rusu, Evaluation of the wave energy conversion efficiency in various coastal environments, *Energies* 7 (2014) 4002–4018, <https://doi.org/10.3390/en7064002>.
- [14] C.V.C. Weiss, R. Guanche, B. Ondiviela, O.F. Castellanos, J. Juanes, Marine renewable energy potential: a global perspective for offshore wind and wave exploitation, *Energy Convers. Manag.* 177 (2018) 43–54, <https://doi.org/10.1016/j.enconman.2018.09.059>.
- [15] R. Guanche, A. De Andrés, I.J. Losada, C. Vidal, A global analysis of the operation and maintenance role on the placing of wave energy farms, *Energy Convers. Manag.* 106 (2015) 440–456, <https://doi.org/10.1016/j.enconman.2015.09.022>.
- [16] N. Guillou, G. Lavidas, G. Chapalain, Wave energy resource assessment for exploitation-A review, *J. Mar. Sci. Eng.* 8 (2020), <https://doi.org/10.3390/JMSE8090705>.
- [17] L. Margheritini, J.P. Kofoed, Weptos wave energy converters to cover the energy needs of a small island, *Energies* 12 (2019), <https://doi.org/10.3390/en12030423>.
- [18] E. Rusu, F. Onea, An assessment of the wind and wave power potential in the island environment, *Energy* 175 (2019) 830–846, <https://doi.org/10.1016/j.energy.2019.03.130>.
- [19] E. Rusu, F. Onea, A parallel evaluation of the wind and wave energy resources along the Latin American and European coastal environments, *Renew. Energy* 143 (2019) 1594–1607, <https://doi.org/10.1016/j.renene.2019.05.117>.
- [20] G. Iglesias, R. Carballo, Wave power for La isla bonita, *Energy* 35 (2010) 5013–5021, <https://doi.org/10.1016/j.energy.2010.08.020>.
- [21] G. Iglesias, R. Carballo, Wave resource in El Hierro d an island towards energy self-sufficiency, *Renew. Energy* 36 (2011) 689–698, <https://doi.org/10.1016/j.renene.2010.08.021>.
- [22] J.P. Sierra, D. González-Marco, J. Sospedra, X. Gironella, C. Mösso, A. Sánchez-Arcilla, Wave energy resource assessment in Lanzarote (Spain), *Renew. Energy* 55 (2013) 480–489, <https://doi.org/10.1016/j.renene.2013.01.004>.
- [23] M. Veigas, G. Iglesias, Wave and offshore wind potential for the island of Tenerife, *Energy Convers. Manag.* 76 (2013) 738–745, <https://doi.org/10.1016/j.enconman.2013.08.020>.
- [24] International Electrotechnical Commission (IEC), *Wave Energy Resource Assessment and Characterization*, Technical report, Geneva, Switzerland, 2014.
- [25] M. Veigas, R. Carballo, G. Iglesias, Energy for Sustainable Development Wave and Offshore Wind Energy on an Island, 22, *Energy for Sustainable Development*, 2014, pp. 57–65, <https://doi.org/10.1016/j.esd.2013.11.004>.
- [26] D.V. Bertram, A.H. Tarighaleslami, M.R.W. Walmsley, M.J. Atkins, G.D.E. Glasgow, A systematic approach for selecting suitable wave energy converters for potential wave energy farm sites, *Renew. Sustain. Energy Rev.* 132 (2020) 110011, <https://doi.org/10.1016/j.rser.2020.110011>.
- [27] C.M. Service, Atlantic Iberian Biscay Irish- Ocean Wave Reanalysis, 2020, https://resources.marine.copernicus.eu/?option=com_csw&view=details&product_id=IBI_MULTITYEAR_WAV_005_006.
- [28] P.Y. Le Traon, A. Reppucci, E. Alvarez Fanjul, L. Aouf, A. Behrens, M. Belmonte, A. Bentamy, L. Bertino, V.E. Brandt, M.B. Kreiner, M. Benkiran, T. Carval, S.A. Ciliberti, H. Clautre, E. Clementi, G. Coppini, G. Cossarini, M. De Alfonso Alonso-Muñoz, A. Delamarche, G. Dibarbour, F. Dinessen, M. Drevillon, Y. Drillet, Y. Faugere, V. Fernández, A. Fleming, M.I. Garcia-Hermosa, M.G. Sotillo, G. Garric, F. Gasparin, C. Giordan, M. Gehlen, M.L. Gregoire, S. Guinehut, M. Hamon, C. Harris, F. Hernandez, J.B. Hinkler, J. Hoyer, J. Karvonen, S. Kay, R. King, T. Lavergne, B. Lemieux-Dudon, L. Lima, C. Mao, M.J. Martin, S. Masina, A. Melet, B. Buongiorno Nardelli, G. Nolan, A. Pascual, J. Pistoia, A. Palazov, J.F. Piolle, M.I. Pujol, A.C. Pequignet, E. Peneva, B. Pérez Gómez, L. Petit de la Villeon, N. Pinardi, A. Pisano, S. Pouliquen, R. Reid, E. Remy, R. Santoleri, J. Siddorn, J. She, J. Staneva, A. Stoffelen, M. Tonani, L. Vandenbulcke, K. von Schuckmann, G. Volpe, C. Wettre, A. Zacharioudaki, From observation to information and users: the Copernicus marine Service perspective, *Front. Mar. Sci.* 6 (2019), <https://doi.org/10.3389/fmars.2019.00234>.
- [29] C. Lorea, G. San, E.B. Rodríguez, C. Toledano, A. Dalphinnet, L. Aouf, P. Lorente, M. De Alfonso, M.G. Sotillo, M. Alfonso, R. Renaud, C. Toledano, P. Lorente, L. Aouf, M. Alfonso, R. Renaud, M. Alfonso, M. Alfonso, M. Alfonso, Atlantic Iberian Biscay Irish- IBI Production Centre, 2020.
- [30] C.B. Levier, P. Lorente, G. Refray, M. Sotillo, B. Levier, M.G. Sotillo, M.G. Sotillo, M.G. Sotillo, E. Alvarez, L. Crosnier, Atlantic Iberian Biscay Irish- IBI production centre. IBI_MULTITYEAR_PHY_005_002. Quality Information Document, Marine Environment Monitoring Service, COPERNICUS, 2021.
- [31] N.N.G.D. Center, ETOPO1 1 Arc-Minute Global Relief Model, NOAA National Centers for Environmental Information., 2020 (n.d.).
- [32] B.G. Reguero, I.J. Losada, F.J. Méndez, A global wave power resource and its seasonal, interannual and long-term variability, *Appl. Energy* 148 (2015) 366–380, <https://doi.org/10.1016/j.apenergy.2015.03.114>.
- [33] G. Iglesias, R. Carballo, Wave energy resource in the Estaca de Bares area (Spain), *Renew. Energy* 35 (2010) 1574–1584, <https://doi.org/10.1016/j.renene.2009.10.019>.
- [34] International Electrotechnical Commission (IEC), *International Electrotechnical Commission, Marine Energy - Wave, Tidal and Other Water Current Converters - Part 1, Terminology*, Geneva, Switzerland, 2011.
- [35] M.R.D. Quitaras, M.L.S. Abundo, L.A.M. Danao, A techno-economic assessment of wave energy resources in the Philippines, *Renew. Sustain. Energy Rev.* 88 (2018) 68–81, <https://doi.org/10.1016/j.rser.2018.02.016>.
- [36] R. Read, H. Bingham, Time- and frequency-domain comparisons of the wavepiston wave energy converter, in: 33rd International Workshop on Water Waves and Floating Bodies (IWWWFB 2018), Guidel-Plages, France, 2018 n. n. pag. <http://orbit.dtu.dk/files/148170140/report.pdf>. (Accessed 16 April 2019).
- [37] O. Choupin, F. Pinheiro Andutta, A. Etemad-Shahidi, R. Tomlinson, A decision-making process for wave energy converter and location pairing, *Renew. Sustain. Energy Rev.* 147 (2021) 111225, <https://doi.org/10.1016/j.rser.2021.111225>.
- [38] S. Foteinis, J. Hancock, N. Mazarakis, T. Tsoutsos, C.E. Synolakis, A comparative analysis of wave power in the nearshore by WAM estimates and in-situ (AWAC) measurements. The case study of Varkiza, Athens, Greece, *Energy* 138 (2017) 500–508, <https://doi.org/10.1016/j.energy.2017.07.061>.
- [39] M.A. Hemer, I. Simmonds, K. Keay, A classification of wave generation characteristics during large wave events on the Southern Australian margin, *Continent. Shelf Res.* 28 (2008) 634–652, <https://doi.org/10.1016/j.csr.2007.12.004>.
- [40] Z. Demirebilek, C.L. Vincent, *Water Wave Mechanics, Chapter 1 EM 1110-2-1100 Part 2, Coastal Engineering Manual*, 2002, pp. 1–127.
- [41] W. Sheng, H. Li, A method for energy and resource assessment of waves in finite water depths, *Energies* 10 (2017) 460, <https://doi.org/10.3390/en10040460>.
- [42] B. Le Méhauté, Linear small amplitude wave theories, in: B. Le Méhauté (Ed.), *An Introduction to Hydrodynamics and Water Waves*, Springer, Berlin, Heidelberg, 1976, pp. 212–238, https://doi.org/10.1007/978-3-642-85567-2_16.
- [43] R.G. Dean, R.A. Dalrymple, *Water Wave Mechanics for Engineers and Scientists*, World Scientific Publishing Company, 1991.
- [44] M. Monteforte, C. Lo Re, G.B. Ferreri, Wave energy assessment in Sicily (Italy), *Renew. Energy* 78 (2015) 276–287, <https://doi.org/10.1016/j.renene.2015.01.006>.
- [45] Stuhlmeier Raphael, Dali Xu, WEC design based on refined mean annual energy production for the Israeli mediterranean coast, *J. Waterw. Port. Coast. Ocean Eng.* 144 (2018), 06018002, [https://doi.org/10.1061/\(ASCE\)JWW.1943-5460.0000451](https://doi.org/10.1061/(ASCE)JWW.1943-5460.0000451).
- [46] N. Arean, R. Carballo, G. Iglesias, An integrated approach for the installation of a wave farm, *Energy* 138 (2017) 910–919, <https://doi.org/10.1016/j.energy.2017.07.114>.
- [47] B. Kamranzad, K. Takara, A climate-dependent sustainability index for wave energy resources in Northeast Asia, *Energy* 209 (2020) 118466, <https://doi.org/10.1016/j.energy.2020.118466>.
- [48] G. Lavidas, Selection index for Wave Energy Deployments (SIWED): a near-

- deterministic index for wave energy converters, *Energy* 196 (2020) 117131, <https://doi.org/10.1016/j.energy.2020.117131>.
- [49] G. Lavidas, B. Kamranzad, Assessment of wave power stability and classification with two global datasets, *Int. J. Sustain. Energy* (2020) 1–16, <https://doi.org/10.1080/14786451.2020.1821027>, 0.
- [50] A. Martínez, G. Iglesias, Wave exploitability index and wave resource classification, *Renew. Sustain. Energy Rev.* 134 (2020) 110393, <https://doi.org/10.1016/j.rser.2020.110393>.
- [51] R.G. Coe, S. Ahn, V.S. Neary, P.H. Kobos, G. Bacelli, Maybe less is more: considering capacity factor, saturation, variability, and filtering effects of wave energy devices, *Appl. Energy* 291 (2021) 116763, <https://doi.org/10.1016/j.apenergy.2021.116763>.
- [52] P. Berens, CirsSat: a matlab toolbox for circular statistics, *J. Stat. Software* 31 (2009) 1–12.
- [53] S. Díaz, J.A. Carta, A. Castañeda, Influence of the variation of meteorological and operational parameters on estimation of the power output of a wind farm with active power control, *Renew. Energy* 159 (2020) 812–826, <https://doi.org/10.1016/j.renene.2020.05.187>.
- [54] A. Cornett, A global wave energy resource assessment, *Sea Technol.* 50 (2009) 59–64.
- [55] I. Fairley, M. Lewis, B. Robertson, M. Hemer, I. Masters, J. Horrillo-Caraballo, H. Karunarathna, D.E. Reeve, A classification system for global wave energy resources based on multivariate clustering, *Appl. Energy* 262 (2020) 114515, <https://doi.org/10.1016/j.apenergy.2020.114515>.
- [56] M. Gonçalves, P. Martinho, C. Guedes Soares, A 33-year hindcast on wave energy assessment in the western French coast, *Energy* 165 (2018) 790–801, <https://doi.org/10.1016/j.energy.2018.10.002>.
- [57] B. Kamranzad, K. Takara, A climate-dependent sustainability index for wave energy resources in Northeast Asia, *Energy* 209 (2020) 118466, <https://doi.org/10.1016/j.energy.2020.118466>.
- [58] B. Kamranzad, A. Etamad-Shahidi, V. Chegini, Developing an optimum hot-spot identifier for wave energy extracting in the northern Persian Gulf, *Renew. Energy* 114 (2017) 59–71, <https://doi.org/10.1016/j.renene.2017.03.026>.
- [59] S. Ahn, K.A. Haas, V.S. Neary, Wave energy resource characterization and assessment for coastal waters of the United States, *Appl. Energy* 267 (2020) 114922, <https://doi.org/10.1016/j.apenergy.2020.114922>.
- [60] Y. Demir, Ö.C. Bilgin, Application of Circular Statistics to Life Science, 2019, <https://www.semanticscholar.org/paper/Application-of-circular-statistics-to-life-science-Demir-Bilgin/c4525b5be3c5c90ef783a3b0513600ce5ef18dd8>. (Accessed 7 October 2021).
- [61] M. Mathiesen, Y. Goda, P.J. Hawkes, E. Mansard, M.J. Martín, E. Peltier, E.F. Thompson, G. Van Vledder, Methodes conseillées pour l'analyse des houles extreme, *J. Hydraul. Res.* 32 (1994) 803–814, <https://doi.org/10.1080/00221689409498691>.
- [62] Y. Goda, *Random Seas and Design of Maritime Structures*, World Scie, 2010.
- [63] G. Lavidas, Wave Energy Resource Modelling and Energy Pattern Identification Using a Spectral Wave Model, Doctor of Philosophy, The university of Edinburgh, 2016. <http://hdl.handle.net/1842/25506>.
- [64] J.W. Kamphuis, Introduction to Coastal Engineering and Management, World Scientific, 2010.
- [65] P. Embrechts, C. Klüppelberg, T. Mikosch, Modelling Extremal Events: for Insurance and Finance, Springer-Verlag, Berlin Heidelberg, 1997, <https://doi.org/10.1007/978-3-642-33483-2>.
- [66] S. Kotz, S. Nadarajah, *Extreme Value Distributions: Theory and Applications*, Imperial College Press, 2000.
- [67] B. Kamranzad, S. Hadadpour, A multi-criteria approach for selection of wave energy converter/location, *Energy* 204 (2020) 117924, <https://doi.org/10.1016/j.energy.2020.117924>.
- [68] K. Mangor, *Shoreline Management Guidelines*, DHI Water & Environment, 2004.
- [69] T. Johannessen, S. Haver, T. Bunnik, B. Buchner, Extreme wave effects on deep water Tlps lessons learned from the Snorre a model tests, *Proc. Deep Offshore Techno.* (2006) 28–30, 2006.
- [70] L. Rusu, F. Onea, The performance of some state-of-the-art wave energy converters in locations with the worldwide highest wave power, *Renew. Sustain. Energy Rev.* 75 (2017) 1348–1362, <https://doi.org/10.1016/j.rser.2016.11.123>.
- [71] M. O'Connor, T. Lewis, G. Dalton, Weather window analysis of Irish west coast wave data with relevance to operations & maintenance of marine renewables, *Renew. Energy* 52 (2013) 57–66, <https://doi.org/10.1016/j.renene.2012.10.021>. In press.
- [72] QGIS development team, QGIS Geographic Information System, Open Source Geospatial Foundation, 2018. <https://qgis.org/es/site/>. April 27, 2021).
- [73] H. Diaz, C.G. Soares, A multi-criteria approach to evaluate floating offshore wind farms siting in the canary islands (Spain), *Energies* 14 (2021) 865, <https://doi.org/10.3390/en14040865>.
- [74] Ministerio para la transición ecológica y el reto demográfico, Biodiversidad marina. Espacios marinos protegidos, Gobierno de España, 2021. <https://www.miteco.gob.es/gli/biodiversidad/temas/biodiversidad-marina/>.
- [75] Gobierno de Canarias, Infraestructura de datos espaciales de Canarias, 2021 n.d.), <https://www.grafcan.es/>. (Accessed 5 May 2021).
- [76] Dimitris Lekkas, Traffic density maps, Marine Traff. (2021). <https://www.marinetraffic.com/es/ais/home/centerx:-12.0/centery:24.9/zoom:4>. (Accessed 5 June 2021).
- [77] Gobierno de España, Servidumbres aeronauticas. Agencia estatal de seguridad aerea, 2021. <https://www.seguridadaerea.gob.es/>. (Accessed 4 May 2021).
- [78] Inc. Primetrica, Submarine Cable Map, TeleGeography, 2021. <https://www.submarinecablemap.com/>. (Accessed 3 April 2021).
- [79] J.K. Kaldellis, T. Chrysikos, Wave energy exploitation in the Ionian Sea Hellenic coasts: spatial planning of potential wave power stations, *Int. J. Sustain. Energy* 38 (2019) 312–332, <https://doi.org/10.1080/14786451.2018.1539395>.
- [80] L. Castro-Santos, G.P. Garcia, T. Simões, A. Estanqueiro, Planning of the installation of offshore renewable energies: a GIS approach of the Portuguese roadmap, *Renew. Energy* 132 (2019) 1251–1262, <https://doi.org/10.1016/j.renene.2018.09.031>.
- [81] E. Loukogeorgaki, D.G. Vagiona, M. Vasileiou, Site selection of hybrid offshore wind and wave energy systems in Greece incorporating environmental impact assessment, *Energies* 11 (2018), <https://doi.org/10.3390/en11082095>.
- [82] M. Vasileiou, E. Loukogeorgaki, D.G. Vagiona, GIS-based multi-criteria decision analysis for site selection of hybrid offshore wind and wave energy systems in Greece, *Renew. Sustain. Energy Rev.* 73 (2017) 745–757, <https://doi.org/10.1016/j.rser.2017.01.161>.
- [83] J. Schallenberg-Rodríguez, N. García Montesdeoca, Spatial planning to estimate the offshore wind energy potential in coastal regions and islands. Practical case: the Canary Islands, *Energy* 143 (2018) 91–103, <https://doi.org/10.1016/j.energy.2017.10.084>.
- [84] J.F. Chozas, H.C. Soerensen, State of the art of wave energy in Spain, in: 2009 IEEE Electrical Power & Energy Conference (EPEC), IEEE, 2009, pp. 1–6, <https://doi.org/10.1109/EPEC.2009.5420989>.
- [85] R. Harris, L. Johanning, *Mooring Systems for Wave Energy Converters: A Review of Design Issues and Choices*, 2006.
- [86] S. Xu, S. Wang, C.G. Soares, Review of mooring design for floating wave energy converters, *Renew. Sustain. Energy Rev.* 111 (2019) 595–621, <https://doi.org/10.1016/j.rser.2019.05.027>.
- [87] M. Lehmann, F. Karimpour, A. Goudey, P.T. Jacobson, Ocean Wave Energy in the United States : Current Status and Future Perspectives, 74, 2017, pp. 1300–1313, <https://doi.org/10.1016/j.rser.2016.11.101>.
- [88] PLASMAR+ Project, Progress of Sustainable Planning of Marine Areas in Macaronesia, 2021. <https://www.plasmar.eu/>. April 27, 2021).
- [89] United Nations, Montego Bay International Law of the Sea Convention, 1982. https://treaties.un.org/Pages/ViewDetailsIII.aspx?src=TREATY&mtldsg_no=XXI-6&chapter=21&Temp=mtldsg3&clang=en. (Accessed 25 April 2021).
- [90] N.K. Losada, I. J. C.V. Pascual, F.J.M. Incera, R.M. Solana, S.R. Landeira, P.C. Braña, A.T. Sampedro, et al., Evaluación del potencial de la energía de las olas, *Estudio Técnico PER*, 2011.
- [91] J. Carrillo, J.C. Guerra, E. Cuevas, J. Barrancos, Characterization of the marine boundary layer and the trade-wind inversion over the sub-tropical north atlantic, *Boundary-Layer Meteorol.* 158 (2016) 311–330, <https://doi.org/10.1007/s10546-015-0081-1>.
- [92] A.M. Cornett, A Global Wave Energy Resource Assessment, in: *Eighteenth International Offshore and Polar Engineering Conference*, Vancouver, 2008.
- [93] S. Bozzi, M. Giassi, A. Moreno Miquel, A. Antonini, F. Bizzozero, G. Grusso, R. Archetti, G. Passoni, Wave energy farm design in real wave climates: the Italian offshore, *Energy* 122 (2017) 378–389, <https://doi.org/10.1016/j.energy.2017.01.094>.
- [94] S.R. Massel, On the largest wave height in water of constant depth, *Ocean Eng.* 23 (1996) 553–573, [https://doi.org/10.1016/0029-8018\(95\)00049-6](https://doi.org/10.1016/0029-8018(95)00049-6).
- [95] N.H. Idris, Wave energy resource assessment with improved satellite altimetry data over the Malaysian coastal sea, *Arabian J. Geosci.* 12 (2019), <https://doi.org/10.1007/s12517-019-4670-z>.
- [96] B. Soudan, Community-scale baseload generation from marine energy, *Energy* 189 (2019) 116134, <https://doi.org/10.1016/j.energy.2019.116134>.
- [97] F. Aristodemo, D. Algeri Ferraro, Feasibility of WEC installations for domestic and public electrical supplies: a case study off the Calabrian coast, *Renew. Energy* 121 (2018) 261–285, <https://doi.org/10.1016/j.renene.2018.01.012>.
- [98] G. Lavidas, K. Blok, Shifting wave energy perceptions: the case for wave energy converter (WEC) feasibility at milder resources, *Renew. Energy* 170 (2021) 1143–1155, <https://doi.org/10.1016/j.renene.2021.02.041>.
- [99] J. Portilla, J. Sosa, L. Cavaleri, Wave energy resources: wave climate and exploitation, *Renew. Energy* 57 (2013) 594–605, <https://doi.org/10.1016/j.renene.2013.02.032>.
- [100] N. Guillou, G. Chapalain, Annual and seasonal variabilities in the performances of wave energy converters, *Energy* 165 (2018) 812–823, <https://doi.org/10.1016/j.energy.2018.10.001>.
- [101] J. Morim, N. Cartwright, M. Hemer, A. Etamad-Shahidi, D. Straus, Inter- and intra-annual variability of potential power production from wave energy converters, *Energy* 169 (2019) 1224–1241, <https://doi.org/10.1016/j.energy.2018.12.080>.
- [102] N. Guillou, G. Chapalain, Assessment of wave power variability and exploitation with a long-term hindcast database, *Renew. Energy* 154 (2020) 1272–1282, <https://doi.org/10.1016/j.renene.2020.03.076>.
- [103] S. Díaz, J.A. Carta, A. Castañeda, Influence of the variation of meteorological and operational parameters on estimation of the power output of a wind farm with active power control, *Renew. Energy* 159 (2020) 812–826, <https://doi.org/10.1016/j.renene.2020.05.187>.
- [104] L. Cuadra, I. Ocampo-Estrella, E. Alexandre, S. Salcedo-Sanz, A study on the

- impact of easements in the deployment of wind farms near airport facilities, *Renew. Energy* 135 (2019) 566–588, <https://doi.org/10.1016/j.renene.2018.12.038>.
- [105] J. De Parscau, *Cumulative Impact of Marine Renewable Energy*, 2011. *Engineering*.
- [106] W.J. Grecian, R. Inger, M.J. Attrill, S. Bearhop, B.J. Godley, M.J. Witt, S.C. Votier, Potential impacts of wave-powered marine renewable energy installations on marine birds, *Ibis* 152 (2010) 683–697, <https://doi.org/10.1111/j.1474-919X.2010.01048.x>.
- [107] M.J. Witt, E.V. Sheehan, S. Bearhop, A.C. Broderick, D.C. Conley, S.P. Cotterell, E. Crow, W.J. Grecian, C. Halsband, D.J. Hodgson, P. Hosegood, R. Inger, P.I. Miller, D.W. Sims, R.C. Thompson, K. Vanstaen, S.C. Votier, M.J. Attrill, B.J. Godley, Assessing wave energy effects on biodiversity: the Wave Hub experience, *Phil. Trans. Math. Phys. Eng. Sci.* 370 (2012) 502–529, <https://doi.org/10.1098/rsta.2011.0265>.
- [108] Government of Spain, Important Community Places in Terms of Habitats-Eszz15002-Marine Area of the East and South of Lanzarote and Fuerteventura, 2021. <https://www.miteco.gob.es/es/costas/temas/proteccion-costa/actuaciones-proteccion-costa/las-palmas/LIC-ESZZ15002-Oriente-Sur-Lanzarote-Fuerteventura.aspx>, June 15, 2021).
- [109] B. Wilson, R.S. Batty, F. Daunt, C. Carter, *Collision Risks between Marine Renewable Energy Devices and Mammals, Fish and Diving Birds Report to the Scottish Executive*, 2007, pp. 1–105.
- [110] K. Haikonen, J. Sundberg, M. Leijon, Characteristics of the operational noise from full scale wave energy converters in the Lysekil project: estimation of potential environmental impacts, *Energies* 6 (2013) 2562–2582, <https://doi.org/10.3390/en6052562>.
- [111] M. Apolonia, T. Simas, Life cycle assessment of an oscillating wave surge energy converter, *J. Mar. Sci. Eng.* 9 (2021) 1–17, <https://doi.org/10.3390/JMSE9020206>.
- [112] J.E. Stopa, K.F. Cheung, Intercomparison of wind and wave data from the ECMWF reanalysis interim and the NCEP climate forecast system reanalysis, *Ocean Model.* 75 (2014) 65–83, <https://doi.org/10.1016/j.ocemod.2013.12.006>.
- [113] L. Rusu, F. Onea, Assessment of the performances of various wave energy converters along the European continental coasts, *Energy* 82 (2015) 889–904, <https://doi.org/10.1016/j.energy.2015.01.099>.
- [114] M. Gonçalves, P. Martinho, C. Guedes Soares, A 33-year hindcast on wave energy assessment in the western French coast, *Energy* 165 (2018) 790–801, <https://doi.org/10.1016/j.energy.2018.10.002>.
- [115] D. Chan, J. Mo, Life cycle reliability and maintenance analyses of wind turbines, *Energy Proc.* 110 (2017) 328–333, <https://doi.org/10.1016/j.egypro.2017.03.148>.
- [116] S. Behrens, J. Hayward, M. Hemer, P. Osman, Assessing the wave energy converter potential for Australian coastal regions, *Renew. Energy* 43 (2012) 210–217, <https://doi.org/10.1016/j.renene.2011.11.031>.
- [117] S. Behrens, J.A. Hayward, S.C. Woodman, M.A. Hemer, M. Ayre, Wave energy for Australia's national electricity market, *Renew. Energy* 81 (2015) 685–693, <https://doi.org/10.1016/j.renene.2015.03.076>.